REFERENCES

Anquetil, P.A., Yu, H., Madden, J.D., Madden, P.G., Swager, T.M., and Hunter, I.W. (2002) Thiophene-based conducting polymer molecular actuators. Proceedings of SPIE, 4695, 424-434.

Boochathum, P., and Prajudtake, W. (2001) Vulcanization of *cis*- and *trans*-polyisoprene and their blends: cure characteristics and crosslink distribution. European Polymer Journal, 37, 417-427.

Chandrasekhar, P. (1999) Fundamnetals and Applications of Conducting Polymers Handbook, USA: Kluwer Academic Publishers.

Choi, S-S. (1999) Correlation of crosslink density with pyrolysis pattern of natural Rubber vulcanizates with efficient vulcanizing cure system. Journal of Analytical and Applied Pyrolysis, 52, 105-112.

Chotpattananont, D., Sirivat, A., and Jamieson, A.M. (2004) Electrorheological properties of perchloric acid-doped polythiophene suspensions. Colloid Polym Sci, 282, 357-365.

Davidson, K., and Ponsonby, A.M. (1999) Synthesis of cross-linked electrically conductive polymers. Synthetic Metals, 102, 1512-1513.

Deependra, K., Shahid, A., and Seungyong, Y. (2004) Semiconducting and Metallic Polymers. Condensed matter physics II, 1-19.

Demanze, F., Yassar, A., and Garnier, F. (1996) Alternating Donor-Acceptor Substitutions in Conjugated Polythiophenes. Macromolecules, 29, 4267-4273.

Faez, R., and De Paoli, M-A. (2001) A conductive rubber based on EPDM and Polyaniline I. Dopping method effect. European Polymer Journal, 37, 1139-1143.

Faez, R., Schuster, R-H., and De Paoli, M-A. (2002) A conductive elastomer based on EPDM and polyaniline II. Effect of the crosslinking method. European Polymer Journal, 38, 2459-2463.

Groenendaal, L., Jonas, F., Freitag, D., Pielartzik, H., and Reynolds, J.R. (2000) Poly(3,4-ethylenedioxythiophene) and Its Derivatives: Past, Present, and Future. Advanced Materials, 12, 481-494.

Grulke, E.A. Solubility Parameter Values. Polymer Handbook Volume 2, Brandrup & Immernut Publisher, 519-552.

Holmes, A.B., Peter, L., Sano, T., Morrison, J.J., Feeder, N., and Kraft, A (2001) Supramolecular assemblies with dithieno [3, 2-b;2', 3'-d] thiophenes and other conjugated thiophene-containing π-systems. Synthetic Metals, 119, 175-176.

Horkay, F., McKenna, G.B., Deschamps, P., and Geissler, E. (2000) Neutron Scattering Properties of Randomly Crosslinked Polyisoprene Gels. Macromolecules, 33, 5215-5220.

Huang, J., Miller, P.F., Wilson, J.S., de Mello, A.J., de Mello, J.C., and Bradley, D.D.C. (2005) Investigation of the Effect of Doping and Post-Deposition Treatments on the Conductivity, Morphology, and Work Function of Poly(3,4-ethylenedioxythiophene)/Poly(styrene sulfonate) Films. Advanced Functional Materials, 15, 290-296.

Jacqueline, I.K. (1990) Concise Encyclopedia of Polymer Science and Engineering. 2nd edition. New York: A Wiley-Interscience Publication.

Jönsson, S.K.M., Birgerson, J., Crispin, X., Greczynski, G., Osikowicz, W., Denier van der Gon, A.W., Salaneck, W.R., Fahlman, M. (2003) The Effect of solvents on the morphology and sheet resistance in poly(3,4-ethylenedioxythiophene)-polystylenesulfonic acid (PEDOT-PSS) films. Synthetic Metals, 139, 1-10.

Kawai, T., Tanaka, F., Kojima, S., and Yoshino, K. (1999) Electrical and optical properties of poly(3-alkoxythiophen) andtheir application for gas sensor. Synthetic Metals, 102, 1358-1359.

Khan, I.M., Waugaman, M., Sannigrahi, B., and McGeady, P. (2003) Synthesis, characterization and biocompatibility studies of oligosiloxane modified polythiophenes. European Polymer Journal, 39, 1405-1412.

Kim, B., Chen, L., Gong, J.P., and Osada, Y. (1999) Titration Behavior and Spectral Transitions of Water-Soluble Polythiophene Carboxylic Acids Macromolecules, 32, 3964-3969.

Kim, B., Chen, L., Gong, J.P., Nishino, M., and Osada, Y. (2000) Environmental Responses of Polythiophene Hydrogels. Macromolecules, 33, 1232-1236.

Kim, B., Fukuoka, H., Gong, J.P., and Osada, Y. (2001) Titration Behavior and Spectral Transitions of hydrophobically modified water-soluble polythiophenes. European Polymer Journal, 37, 2499-2503.

Kim, S.R., Choi, S.A., Kim, J.D., Lee, C., Rhee, S.B., and Kim, K.J. (1995) Preparation of polythiophene LB films and their gas sensitivities by the quartz crystal microbalance. Synthetic Metals, 71, 2027-2028.

Knite, M., Teteris, V., Kiploka, A., and Kaupuzs, J. (2004) Polyisoprene-carbon Black nanocomposites as tensile strain and pressure sensor materials. Sensors and Actuators A, 110, 142-149.

Kornbluh, R., Perlrine, R., Joseph, J., Heydt, R., Pei, Q., and Chiba, S. (1999) High-Field Electrostriction of Elastomeric Polymer Dielectrics for Actuation. Proceeding of SPIE, 3669, 149-161.

Krause, S., and Bohon, K. (2001) Electromechanical response of electrorheological fluids and Poly(dimethylsiloxane) networks. Macromolecules, 34, 7179-7189.

Küçükyavuz, S., Sankir, M., and Küçükyavuz, Z. (2002) Electrochemical preparation and characterization of carbon fiber reinforced PDMS/Pth composites. Synthetic Metals, 128, 247-251.

Küçükyavuz, Z., and Kiralp, S. (2003) Preparation and Characterization of Conducting Polybutadiene/Polythiophene Composites. Turk J. Chem, 27, 417-422.

Kumar, D., and Sharma, R.C. (1998) Advances in conductive polymers. European Polymer Journal, 34, 1053-1060.

Lee, C., Kim, K.J., and Rhee, S.B. (1995) The effect of ester substitution and alkyl chain length on the properties of polythiophenes. Synthetic Metals, 69, 295-296.

Liu, B., and Shaw, T.M. (2001) Electrorheology of filled silicone elastomers. Journal of Rheology, 45(3), 641-657.

Louwet, F., Groenendaal, L., Dhane, J., Manca, J., and Luppen, J.V. (2003) PEDOT/PSS: synthesis, characterization, properties and applications. Synthetic Metals, 135-136, 115-117.

McCullough, R.D., and Ewbank, P.C. (1997) Self-Assembly and Chemical

Response of Conducting Polymer Superstructure. Synthetic Metals, 84, 311-312.

Mu, S., and Park, S.M. (1995) Preparation and characterization of polythiophene in aqueous solutions. Synthetic Metals, 69, 311-312.

Nguyen, T.P., Rendu, P.L., Long, P.D., and De Vos, S.A. (2004) Chemical and thermal treatment of PEDOT/PSS thin films for use in organic light emitting diodes. Surface & Coatings Technology, 180-181, 646-649.

Painter, P.C., and Coleman, M.M. (1997) Fundamentals of Polymer Science: An Introductory text, U.S.A: Technomic Publishing Company.

Parthasarathy, M., and Klinggenberg, D.J. (1996) Electrorheology: Mechanisms and Models. Materials Science and Engineering, R17, 57-103.

Raphael, M.O., Samuel, J.H., and Kinam, P. (1996) Hydrogels and Biodegradable Polymer for bioapplications. Washington, D.C: American Chemical Society.

Reedijk, J.A., Martens, H.C.F., van Bohemen, S.M.C., Hilt, O., Brom, H.B., and Michels, M.A.J. (1999) Charge transport in doped polythiophene. Synthetic Metals, 101, 475-476.

Salaneck, W.R., Luncstrom, I., and Ranby, B. (1993) Conjugated polymer and related materials: The interconnection of chemical and electronic structure. New York: Oxford Science Publications.

Shen, Z., Xue, H., and Li, Y. (2001) Polyaniline-polyisoprene composite film Based glucose biosensor with high permselectivity. Synthetic Metals, 124, 345-349.

Shiga, T. (1997) Deformation and Viscoelastic Behavior of Polymer Gels in Electric Fields. Advances in Polymer Science, (134), 131-163.

Stenger-Smith, J.D. (1998) Intrinsically electrically conducting polymers: Synthesis, Characterization, and their applications. Prog. Polym. Sci., 23, 57-79.

Stefan C.J.. Meskers, Jeroen K.J. van Duren, Rene A.J. Janssen. (2004) Non-linearity in the I-V characteristic of poly(3,4-ethylenedioxythiophene): poly(stylenesulfonic acid) (PEDOT/PSS) due to Joule heating. Organic Electronics, 5, 207-211.

Tolbert, L., Edmond, C., and Kowalik, J. (1999) Charge-transfer doping of poly (3-alkyl-2, 2'-bithiophene). Synthetic Metals, 101, 500-501.

Torsi, L., Tafuri, A., Cioffi, N., Gallazzi, M.C., Sassella, A., Sabbatini, L., and Zambonin, P.G. (2003) Regioregular polythiophene field-effect transitors employed as chemical sensors. Sensors and Actuators B, 93, 257-262.

Van Vught, F.A. (2000) Transparent and conductive polymer layers by gas plasma techniques. The Netherlands: L.M.H. Groenewoud.

Wallance, G. G., Small, C. J., and Too, C. O. (1997) Responsive conducting polymer-hydrogel composites. Polymer Gels and Networks, 5, 251-265.

Wang, D.W. (1992) Encyclopedia of Polymer Science and Engineering. 2nd Eddtion, vol. 1. New York: A Wiley-Interscience Publication.

Wang, F., Lai, Y-H., and Han, M-Y. (2004) Stimuli-Responsive Conjugated Copolymers Having Electro-Active Azulene and Bithiophene Units in the Polymer Skeleton: Effect of Protonation and p-Doping on conducting Properties. Macromolecules, 37, 3222-3230.

Wang, T., Qi, Y., Xu, J., Hu, X., and Chen, P. (2005) Effects of poly(ethylene glycol) on electrical conductivity of poly(3,4-ethylenedioxythiophene) -poly(styrenesulfonic acid) film. Applied Surface Science.

Zrínyi, M., Fehér, J., and Filipcsei, G. (2000) Novel gel actuator containing TiO2 particles operated under static electric field. Macromolecules, 33, 5751-5753

APPENDICES

Appendix A: Identification of Characteristic Peaks of FT-IR Spectrum of PEDOT/PSS and Second Doped PEDOT/PSS/EG

FT-IR spectrometer (Thermo Nicolet, Nexus 670) was used to investigate spectra of PEDOT/PSS and PEDOT/PSS/EG. The spectrometer was operated in the absorption mode with 32 scans and a resolution of ±4 cm^{-1}, covering a wave number range of 4000-400 cm^{-1}. Optical grade KBr was used as the background material and the polymers were mixed with dried KBr at a ratio 1:20.

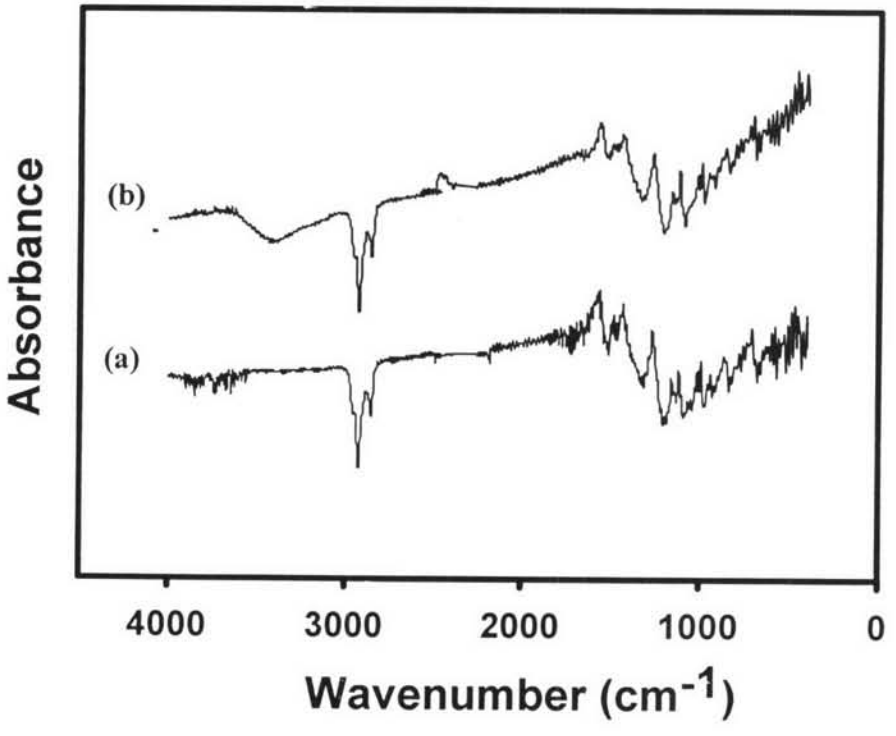

Figure A1 The FT-IR spectra of: a) PEDOT/PSS; b) second doped PEDOT/PSS with EG at volume ratio of PEDOT/PSS to EG unit of 5:1.

In Figure A1, the FT-IR spectrum of PEDOT/PSS, the three absorption peaks at 1588, 1487 and 1395 cm^{-1} can be assigned to the thiophene ring [20]. The peak at 875 cm^{-1} corresponds to the symmetric vibration of C-O-C in cyclic ether structure [20]. These results confirm the existence of PEDOT. Furthermore, the absorption peaks 3000-2800 cm^{-1} is a characteristic absorption peak of polystyrene [21] and its derivative functionalized with the sulfonate groups (SO_3^-) is confirmed by the presence of the peaks at 1203 and 1102 cm^{-1} [20]. Consequently, from the FT-IR spectrum, it indicates the synthesized polymer was a combination of PEDOT and PSS [20, 21]. After second doping with EG, the characteristic peaks of the polyalcohol appeared on FT-IR spectra. There appears a broad peak of hydroxy functional group occurring from 3600 to 3000 cm^{-1}.

Table A1 The FT-IR absorption spectrum of PEDOT/PSS and second doped PEDOT/PSS with EG at volume ratio of PEDOT/PSS to EG unit of 5:1.

Wavenumber (cm^{-1})	**Assignments**	**References**
1588-1487-1395 (1590-1490-1400)	Thiophene ring stretching vibration	Yinghong *et al.* (2004)
875 (878)	C-O-C symmetric vibration	Yinghong *et al.* (2004)
3000-2800	Polystyrene stretching vibration	Christian *et al.* (1986)
1203-1102 (1220-1180)	Sulfonate groups stretching vibration	Yinghong *et al.* (2004)
3600-3000	EG stretching vibration	Christian *et al.* (1986)

Appendix B: The Thermogravimetric Thermogram of PEDOT/PSS and Second Dope PEDOT/PSS/EG

PEDOT/PSS and second doped PEDOT/PSS with EG at 5:1 volume ratio of dopant to polymer unit were determined by a thermal gravimetric analyzer (Pyris Diamond Perkin Elmer). Measurements were carried out with the temperature scan from 30°C to 900°C and a heating rate of 10°C/min. The samples were weighed in the range of 5-20 mg and loaded into a platinum pan, and then it was heated under air flow. Four transitions were observed in PEDOT/PSS, 30-110°C, 160-380°C, 380-560°C and 560-900°C; they can be referred to as the losses of water, the side chain degradation and the polymer backbone degradation. After second doping with EG, we observed five transitions in PEDOT/PSS/EG, 30-140°C, 180-360°C, 360-450°C, 450-600°C and 600-900°C; they can be referred to as the losses of water, the losses of the residual solvent EG, the side chain degradation and the polymer backbone degradation. From the TGA experiments, we observed the existence of the residual EG in the PEDOT/PSS particles.

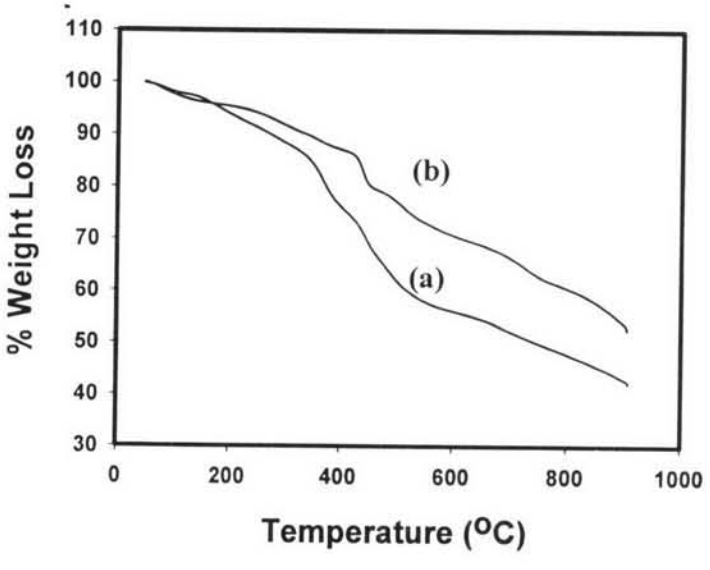

Figure B1 TGA thermograms of: a) PEDOT/PSS; b) second doped PEDOT/PSS/EG at volume ratio of PEDOT/PSS to EG unit of 5:1.

Table B1 Summary of: a) PEDOT/PSS; b) PEDOT/PSS/EG at volume ratio of PEDOT/PSS to EG unit of 5:1. degradation steps

Sample	Transition temperature (°C)					% Weight loss				
	1st	2nd	3rd	4th	5th	1st	2nd	3rd	4th	5th
PEDOT/PSS	30-110	160-380	380-560	560-900	-	3.7	16.8	9.6	20.0	-
PEDOT/PSS/EG	30-140	180-360	360-450	450-600	600-900	2.2	10.2	6.6	4.5	21.5

Appendix C: Determination of the Crystal Lattice Spacing of PEDOT/PSS and PEDOT/PSS/EG by X-ray Diffraction

Powders of polymer were packed onto a glasses plate and data were collected after X-ray passed though the sample. Properties of PEDOT/PSS and PEDOT/PSS/EG were investigated by the peaks of graph. The areas of sharp peak and broad peak can be identified as the crystal part and the amorphous part, respectively.

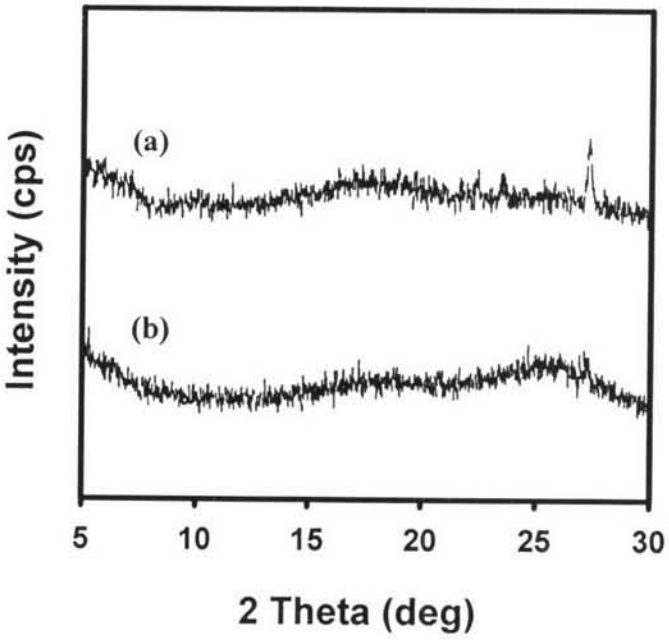

Figure C1 XRD patterns of: a) PEDOT/PSS; b) PEDOT/PSS/EG at volume ratio of PEDOT/PSS: EG unit of 5:1.

From XRD patterns of PEDOT/PSS and PEDOT/PSS/EG, there is no characteristic peak observed by X-ray diffraction. Further evidence is that we observed that all samples are amorphous with short-range structural order. This conformational change of the PEDOT chains in the film may make the backbone pack better, but it does not significantly increase the crystallization of the PEDOT/PSS/EG, so it cannot be

detected by the X-ray diffraction [23]. This is different from the secondary doping of polyaniline [28]. The solvent can affect the conformation of polyaniline chains in solution, so that highly crystalline polyaniline film can be formed when an appropriate solvent is selected.

Appendix D: Scanning Electron Micrograph of PEDOT/PSS, Second Dope PEDOT/PSS/EG and PDMS_PEDOT/PSS Blends

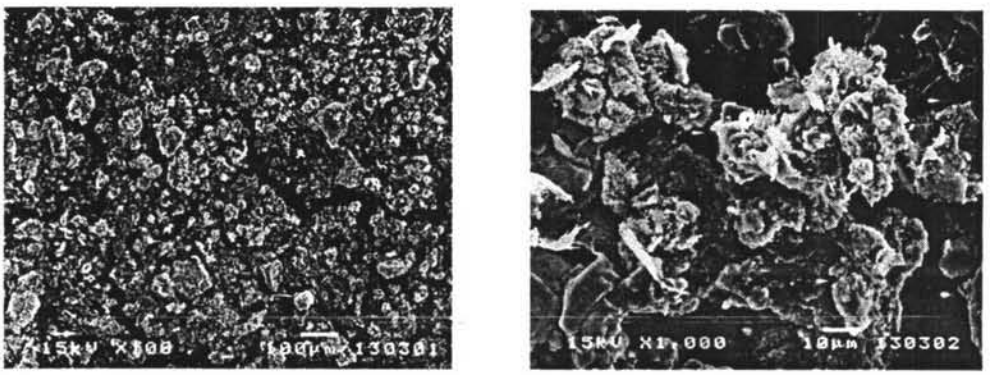

Figure D1 The morphology of PEDOT/PSS at magnification of 100 and 1000.

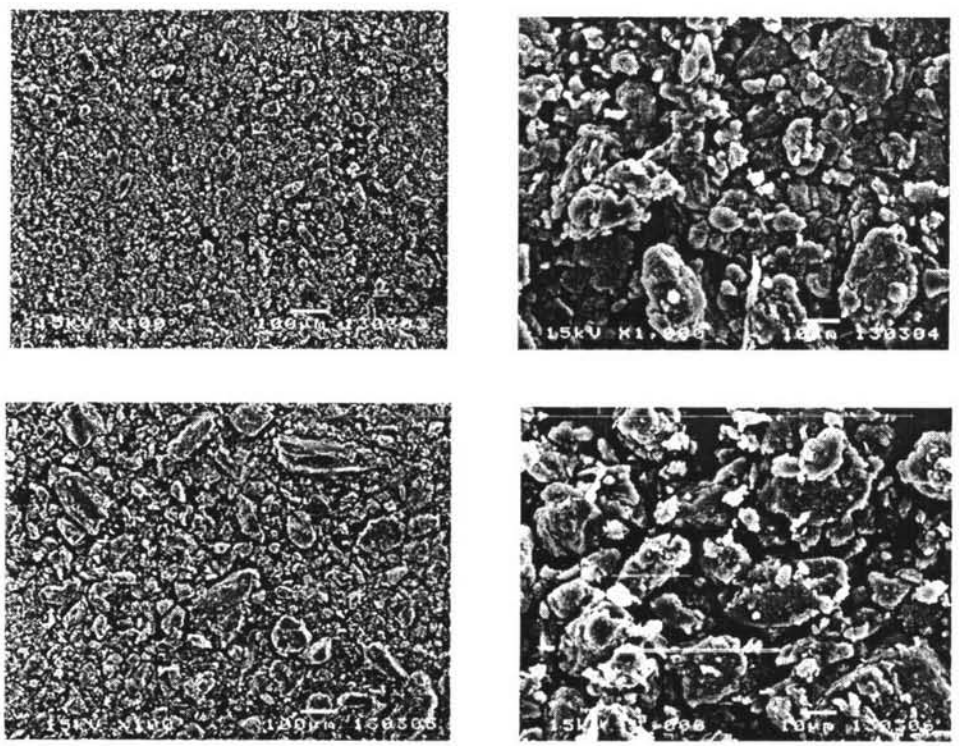

Figure D2 The morphology of second doped PEDOT/PSS/EG powder at volume ratio of PEDOT/PSS to EG unit of 5:1, 5:2, 5:3, 5:4 and 5:5, respectively; at magnifications of 100 and 1000.

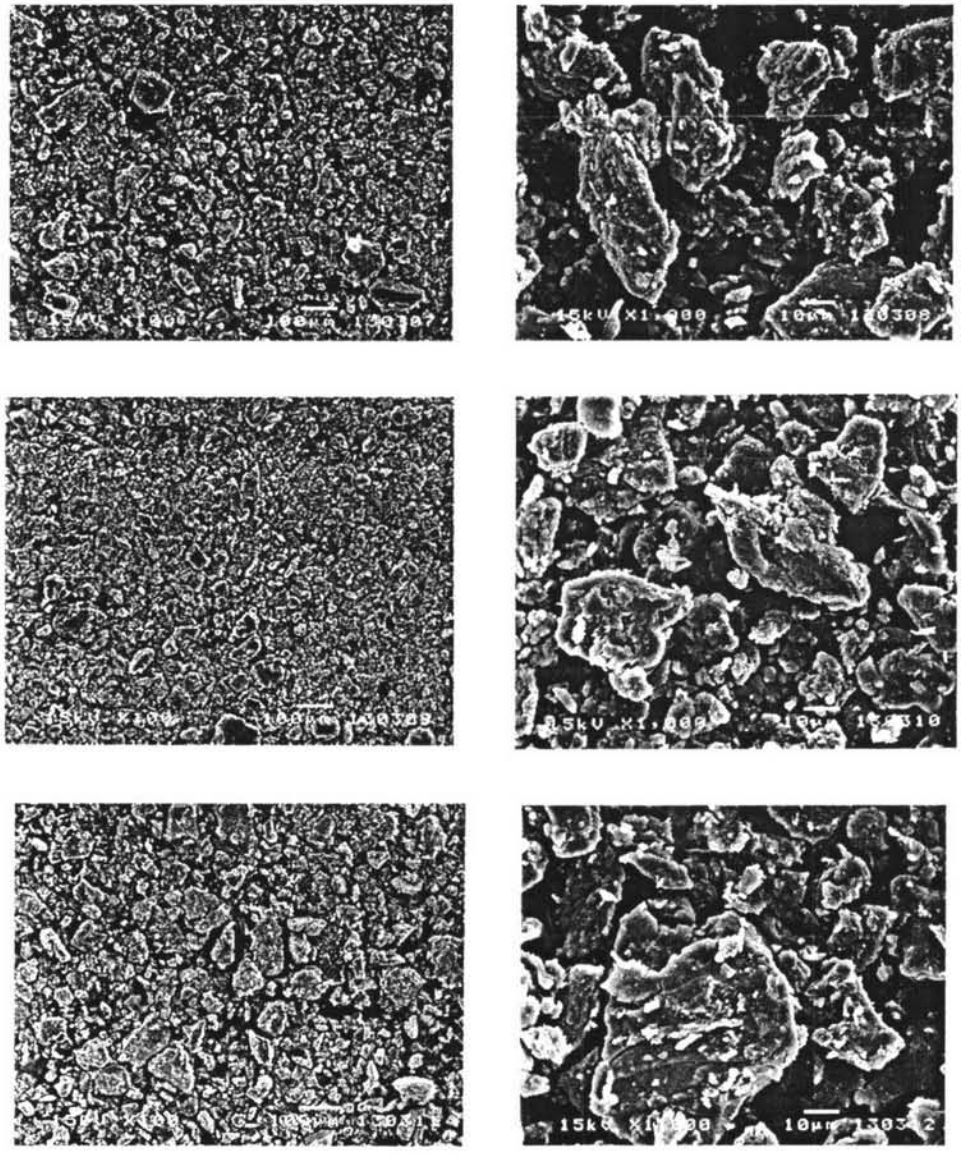

Figure D2(cont.) The morphology of second doped PEDOT/PSS/EG powder at volume ratio of PEDOT/PSS to EG unit of 5:1, 5:2, 5:3, 5:4 and 5:5, respectively; at magnifications of 100 and 1000.

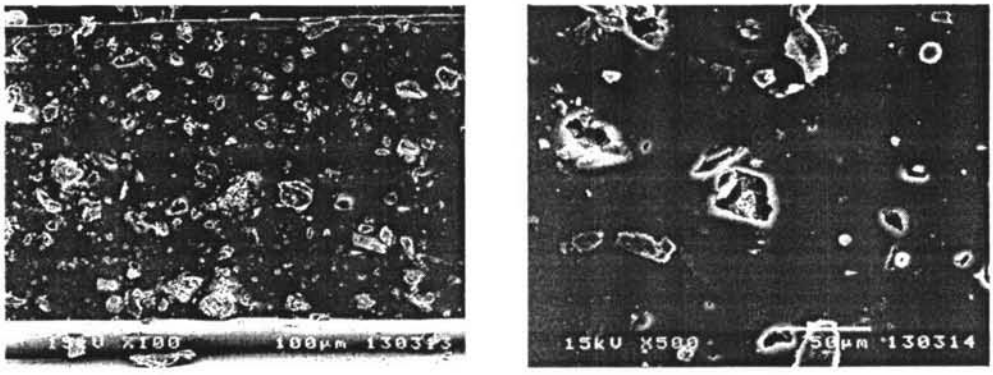

Figure D3 The morphology of PDMS_5%PEDOT/PSS blend at magnifications of 100 and 1000.

Apendix E: Determination of the Correction Factor (K)

The electrical conductivity of conductive polymer was measured by a using two-point probe meter. The surface of sample contact with two point probes of source meter (Keithley, Model 6517A). A constant voltage was applied and a current was measured.

The geometrical correction factor was taken into account of geometric effects, depending on the configuration and probe tip spacing.

$$K = \frac{w}{l} \qquad \text{(E.1)}$$

K is geometrical correction factor, w is width of probe tip spacing (cm), l is the length between probes (cm).

In this measurement, the constant K value was determined by using standard materials where specific resistivity values were known; we used silicon wafer chips (SiO_2). In our case, the sheet resistivity was measured by using our custom made two-point probe and then the geometric correction factor was calculated by equation (E.2) as follows:

$$K = \frac{\rho}{R \times t} = \frac{I \times \rho}{V \times t} \qquad \text{(E.2)}$$

K is geometric correction factor, ρ is resistivity of standard silicon wafer, which was calibrated by using a four point probe at King Mongkut's Institute Technology of Lad Krabang (Ω.cm), t is film thickness (cm), R is film resistance (Ω), I is measure current (A), and V is voltage drop (V).

Standard Si wafers were cleaned to remove organic impurities prior to be used according to the standard RCA method (Kern, 1993).

Materials

Acetones (Scharlau, 99.5%), Methanol (CARLO ERBA, 99.9%), Ammonium hydroxide (Merk, 99.9%), Hydrogen peroxide (CARLO ERBA, 30% in water), and dilute (2%) Hydrofuric acid.

Experiment

The cleaning procedures contain 3 steps: the solvent clean, the RCA01 and the HF dip. The first step is the solvent clean step, employed to remove oils and organic residues that appeared on Si wafer surface. The Si wafer was placed into the acetone at 55°C for 10 min, removed and placed in methanol for 2-5 min, subsequently rinsed with deionized water and blown dried with nitrogen gas. The second step is the RCA clean, to remove organic residues from silicon wafers. This process oxidized the silicon wafer and left a thin oxide on the surface of the wafer. RCA solution was prepared with 5 parts of water (H_2O), 1 part of 27% ammonium hydroxide (NH_4OH), and 1 part of 30% hydrogen peroxide (H_2O_2). 65 ml of NH_4OH (27%) was added into 325 ml of deionized water in a beaker and then heated to 70 ± 5°C. The mixture would bubble vigorously after 1-2 min, indicated that it was ready to use. Silicon wafer was soaked in the solution for 15 min, consequently overflowed with deionized water in order to rinse and remove the solution. The third step is the HF dip, which was carried out to remove native silicon dioxide from wafer. 480 ml of deionised water was added to the polypropylene bottle and then added to 20 ml HF. Wafer was soaked in this solution for 2 min, removed and checked for hydrophobicity by performing the wetting test. Deionized water was poured onto the surface wafer; the clean silicon surface would shows that the beads of water would roll off. Clean Si wafer was further blown dried with nitrogen and stored in a clean and dry environment.

Table E1 Determination the correction factor of four point probe

Probe	K (correction factor)				
	1	2	3	Average	STD
1	1.10E-04	1.09E-04	1.09E-04	1.09E-04	3.05E-07
2	1.60E-05	1.60E-05	1.61E-05	1.61E-05	6.39E-08

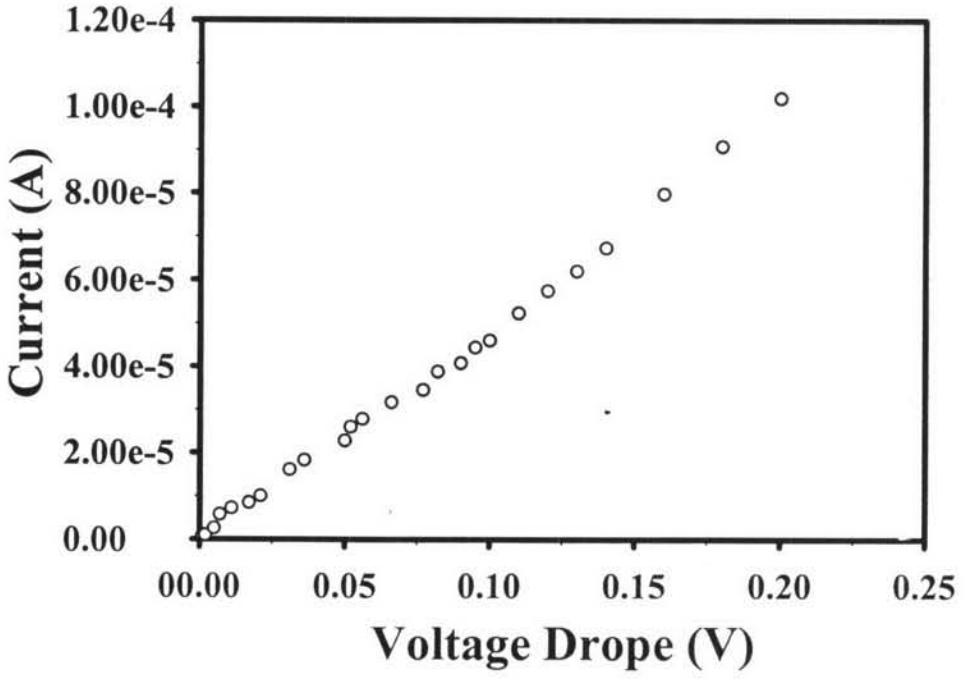

Figure E1 The calibration data of Si-wafer: K tay which specific resistivity (ρ) 0.01647 Ω.cm, thickness 0.0724 cm, 24-25°C, 55-59 %R.H.

Table E2 Determination the correction factor of probe 1 with standard Si wafer (specific resistivity 0.01647 Ω.cm, thickness 0.0724 cm, 24-25°C, 55-59% R.H)

Volt Applied (mV)			Current (mA)		
1	2	3	1	2	3
0.001	0.001	0.001	8.54E-07	8.61E-07	8.33E-07
0.002	0.002	0.002	1.05E-06	1.02E-06	1.02E-06
0.005	0.005	0.005	2.57E-06	2.62E-06	2.62E-06
0.007	0.007	0.007	5.78E-06	5.78E-06	5.77E-06
0.011	0.011	0.011	7.36E-06	7.31E-06	6.98E-06
0.017	0.017	0.017	8.49E-06	8.51E-06	8.57E-06
0.021	0.021	0.021	1.01E-05	1.00E-05	1.00E-05
0.031	0.031	0.031	1.60E-05	1.61E-05	1.62E-05
0.036	0.036	0.036	1.82E-05	1.83E-05	1.83E-05
0.050	0.050	0.050	2.28E-05	2.29E-05	2.26E-05
0.052	0.052	0.052	2.57E-05	2.57E-05	2.57E-05
0.056	0.056	0.056	2.84E-05	2.76E-05	2.75E-05
0.066	0.066	0.066	3.17E-05	3.16E-05	3.16E-05
0.077	0.077	0.077	3.50E-05	3.45E-05	3.41E-05
0.082	0.082	0.082	3.90E-05	3.86E-05	3.86E-05
0.090	0.090	0.090	4.07E-05	4.09E-05	4.09E-05
0.095	0.095	0.095	4.44E-05	4.44E-05	4.43E-05
0.10	0.10	0.10	4.60E-05	4.59E-05	4.60E-05
0.11	0.11	0.11	5.22E-05	5.22E-05	5.23E-05
0.12	0.12	0.12	5.73E-05	5.74E-05	5.74E-05
0.13	0.13	0.13	6.25E-05	6.18E-05	6.16E-05
0.14	0.14	0.14	6.74E-05	6.70E-05	6.74E-05
0.16	0.16	0.16	7.97E-05	7.97E-05	7.96E-05
0.18	0.18	0.18	9.06E-05	9.09E-05	9.07E-05
0.20	0.20	0.20	1.02E-04	1.02E-04	1.02E-04
0.30	0.30	0.30	1.71E-04	1.70E-04	1.70E-04
0.35	0.35	0.35	2.50E-04	2.59E-04	2.55E-04
0.40	0.40	0.40	3.14E-04	3.15E-04	3.15E-04
0.45	0.45	0.45	5.06E-04	4.90E-04	4.90E-04
0.50	0.50	0.50	5.98E-04	6.19E-04	6.14E-04

Table E3 Determination the correction factor of probe 2 with standard Si wafer (specific resistivity 0.01647 Ω.cm, thickness 0.0724 cm, 24-25°C, 55-59% R.H)

Volt Applied (mV)			Current (mA)		
1	2	3	1	2	3
0.005	0.005	0.005	3.14E-07	3.05E-07	3.05E-07
0.01	0.01	0.01	8.28E-07	8.33E-07	8.35E-07
0.02	0.02	0.02	1.37E-06	1.36E-06	1.36E-06
0.03	0.03	0.03	2.09E-06	2.08E-06	2.12E-06
0.04	0.04	0.04	2.81E-06	2.79E-06	2.78E-06
0.05	0.05	0.05	3.44E-06	3.45E-06	3.49E-06
0.06	0.06	0.06	4.36E-06	4.38E-06	4.41E-06
0.07	0.07	0.07	4.99E-06	5.01E-06	5.05E-06
0.08	0.08	0.08	5.64E-06	5.61E-06	5.69E-06
0.09	0.09	0.09	6.41E-06	6.39E-06	6.38E-06
0.10	0.10	0.10	7.21E-06	7.19E-06	7.25E-06
0.11	0.11	0.11	8.20E-06	8.24E-06	8.28E-06
0.12	0.12	0.12	9.30E-06	9.34E-06	9.30E-06
0.13	0.13	0.13	9.96E-06	9.98E-06	1.00E-05
0.14	0.14	0.14	1.09E-05	1.09E-05	1.11E-05
0.15	0.15	0.15	1.19E-05	1.19E-05	1.19E-05
0.20	0.20	0.20	1.63E-05	1.63E-05	1.63E-05
0.25	0.25	0.25	2.21E-05	2.22E-05	2.23E-05
0.30	0.30	0.30	2.84E-05	2.85E-05	2.85E-05
0.35	0.35	0.35	3.63E-05	3.61E-05	3.63E-05

Appendix F: Conductivity Measurement

The specific conductivity can be measured with a two point probe connect to a source meter (Keithley, Model 6517A), and in contact with sample surface and a constant voltage is applied. So a responsive current was measured under the atmospheric pressure, 54-60% relative humidity and 24-25°C. At a responsive current varies linearly does not change with voltage this region is called the linear Ohmic regime which can be identified by plotting the applied voltage versus the current. The applied voltage and the current change in the linear ohmic regime were converted to the electrical conductivity of the polymer by using equation (F.1) as follows:

$$\sigma = \frac{1}{\rho} = \frac{1}{R_s \times t} = \frac{I}{K \times V \times t} \qquad \text{(F.1)}$$

where σ is specific conductivity (S/cm), ρ is specific resistivity (Ω.cm), R_s is sheet resistivity (Ω), I is measure current (A), K is geometric correction factor, V is applied voltage (voltage drop) (V), t is pellet thickness (cm).

In this measurement, the geometric correction factor (K) of probe A is 1.09938×10^{-4} and the thickness of sample pellets was measured by using a thickness gauge.

In addition the conductivity of matrixes can be measured by using the resistivity testing fixture (Keithley, Model 8009) connected to a source meter (Keithley, Model 6517A) for a constant voltage source and reading resultant current under the atmospheric pressure, 54-60% relative humidity and 24-25°C. The conductivity of matrixes can calculate by using equation (F.2 – F.3) as follows:

$$K_v = \frac{\pi \times (D + [\beta \times g])}{4} \qquad \text{(F.2)}$$

where K_v is effective area of the guarded electrode for the particular electrode arrangement employed (cm^2), D is diameter of the guarded electrode (cm), β is effective

area coefficient (cm^2) (β is always zero), g is distance between the guarded electrode and the ring electrode (cm).

$$\sigma = \frac{1}{\rho} = \frac{I}{1.09938\times10^{-4}\times t\times V} \qquad \text{(F.3)}$$

where σ is specific conductivity (S/cm), ρ is specific resistivity (Ω.cm), I is measure current (A), V is applied voltage (voltage drop) (V), t is sheet thickness (cm).

Table F1 Determination the specific conductivity (S/cm) of PEDOT/PSS and second doped PEDOT/PSS with EG.

Code	Specific conductivity (S/cm)		average	STD
PEDOT/PSS	27.9	27.1	27.5	0.6
PEDOT/PSS:EG=5:1	576.0	558.3	563.5	7.6
PEDOT/PSS:EG=5:2	591.9	581.0	586.5	7.7
PEDOT/PSS:EG=5:3	566.1	546.0	556.1	14.2
PEDOT/PSS:EG=5:4	599.1	644.1	621.6	31.8
PEDOT/PSS:EG=5:5	589.7	580.6	585.2	6.4

Table F2 The raw data of the determination of linear regime of PEDOT/PSS at 24-25°C, 54-60% R.H.

Sample	Thickness (cm)	Applied Voltage (V)		Measured Current (A)		Conductivity (S/cm)	
		1	2	1	2	1	2
PEDOT/PSS	1) 0.03272	0.01	0.01	1.0E-06	8.35E-07	2.81E+01	3.02E+01
	2) 0.02512	0.02	0.02	1.6E-06	1.37E-06	2.29E+01	2.49E+01
		0.03	0.03	2.6E-06	2.12E-06	2.45E+01	2.56E+01
		0.04	0.04	3.6E-06	2.86E-06	2.51E+01	2.59E+01
		0.05	0.05	4.6E-06	3.59E-06	2.53E+01	2.60E+01
		0.06	0.06	5.8E-06	4.55E-06	2.70E+01	2.75E+01
		0.07	0.07	6.8E-06	5.26E-06	2.69E+01	2.72E+01
		0.08	0.08	7.8E-06	5.97E-06	2.70E+01	2.70E+01
		0.09	0.09	8.7E-06	6.70E-06	2.70E+01	2.69E+01
		0.1	0.1	9.7E-06	7.42E-06	2.71E+01	2.66E+01
		0.11	0.11	1.1E-05	8.37E-06	2.80E+01	2.76E+01
		0.12	0.12	1.2E-05	9.06E-06	2.78E+01	2.74E+01
		0.13	0.13	1.3E-05	9.79E-06	2.76E+01	2.73E+01
		0.14	0.14	1.4E-05	1.05E-05	2.77E+01	2.71E+01
		0.15	0.15	1.5E-05	1.12E-05	2.78E+01	2.71E+01
		0.16	0.16	1.6E-05	1.22E-05	2.87E+01	2.76E+01
		0.17	0.17	1.7E-05	1.29E-05	2.84E+01	2.76E+01
		0.18	0.18	1.8E-05	1.37E-05	2.85E+01	2.75E+01
		0.19	0.19	2.0E-05	1.44E-05	2.88E+01	2.70E+01
		0.20	0.20	2.1E-05	1.51E-05	2.88E+01	2.73E+01

Table F3 The raw data of the determination of linear regime of second doped PEDOT/PSS with EG at 24-25°C, 51-60 % R.H.

Sample	Thickness (cm)	Applied Voltage (V)		Measured Current (A)		Conductivity (S/cm)	
		1	2	1	2	1	2
5_1	1) 0.02555	0.01	0.01	1.92E-05	1.41E-05	6.82E+02	6.69E+02
	2) 0.01914	0.02	0.02	2.93E-05	2.24E-05	5.22E+02	5.33E+02
		0.03	0.03	4.50E-05	3.44E-05	5.33E+02	5.44E+02
		0.04	0.04	6.09E-05	4.60E-05	5.42E+02	5.46E+02
		0.05	0.05	7.67E-05	5.72E-05	5.46E+02	5.44E+02

Sample	Thickness (cm)	Applied Voltage (V)		Measured Current (A)		Conductivity (S/cm)	
		1	2	1	2	1	2
5_1	1) 0.02555	0.06	0.06	9.76E-05	7.27E-05	5.79E+02	5.76E+02
	2) 0.01914	0.07	0.07	1.13E-04	8.42E-05	5.75E+02	5.72E+02
		0.08	0.08	1.28E-04	9.57E-05	5.71E+02	5.69E+02
		0.09	0.09	1.44E-04	1.08E-04	5.69E+02	5.68E+02
		0.1	0.1	1.59E-04	1.17E-04	5.67E+02	5.57E+02
		0.11	0.11	1.79E-04	1.30E-04	5.81E+02	5.63E+02
		0.12	0.12	1.94E-04	1.39E-04	5.76E+02	5.52E+02
		0.13	0.13	2.09E-04	1.51E-04	5.72E+02	5.51E+02
		0.14	0.14	2.23E-04	1.62E-04	5.68E+02	5.51E+02
		0.15	0.15	2.38E-04	1.70E-04	5.65E+02	5.37E+02
		0.16	0.16	2.58E-04	1.86E-04	5.73E+02	5.53E+02
		0.17	0.17	2.72E-04	1.96E-04	5.69E+02	5.48E+02
		0.18	0.18	2.86E-04	2.06E-04	5.65E+02	5.45E+02
		0.19	0.19	3.00E-04	2.18E-04	5.62E+02	5.44E+02
		0.20	0.20	3.14E-04	2.29E-04	5.60E+02	5.43E+02

Sample	Thickness (cm)	Applied Voltage (V)		Measured Current (A)		Conductivity (S/cm)	
		1	2	1	2	1	2
5_2	1) 0.05139	0.01	0.01	3.58E-05	3.37E-05	6.34E+02	6.80E+02
	2) 0.04513	0.02	0.02	5.78E-05	5.24E-05	5.11E+02	5.28E+02
		0.03	0.03	9.00E-05	8.02E-05	5.31E+02	5.39E+02
		0.04	0.04	1.23E-04	1.08E-04	5.43E+02	5.45E+02
		0.05	0.05	1.56E-04	1.36E-04	5.52E+02	5.49E+02
		0.06	0.06	2.00E-04	1.73E-04	5.90E+02	5.82E+02
		0.07	0.07	2.32E-04	2.01E-04	5.87E+02	5.80E+02
		0.08	0.08	2.66E-04	2.29E-04	5.89E+02	5.78E+02
		0.09	0.09	3.00E-04	2.58E-04	5.90E+02	5.77E+02
		0.1	0.1	3.34E-04	2.85E-04	5.91E+02	5.75E+02
		0.11	0.11	3.78E-04	3.23E-04	6.09E+02	5.91E+02
		0.12	0.12	4.13E-04	3.50E-04	6.09E+02	5.88E+02
		0.13	0.13	4.47E-04	3.78E-04	6.08E+02	5.86E+02
		0.14	0.14	4.81E-04	4.06E-04	6.08E+02	5.85E+02
		0.15	0.15	5.15E-04	4.34E-04	6.08E+02	5.83E+02
		0.16	0.16	5.60E-04	4.71E-04	6.20E+02	5.94E+02
		0.17	0.17	5.93E-04	5.00E-04	6.17E+02	5.92E+02
		0.18	0.18	6.24E-04	5.27E-04	6.13E+02	5.90E+02
		0.19	0.19	6.59E-04	5.55E-04	6.14E+02	5.89E+02
		0.20	0.20	6.92E-04	5.83E-04	6.13E+02	5.88E+02

Sample	Thickness (cm)	Applied Voltage (V)		Measured Current (A)		Conductivity (S/cm)	
		1	2	1	2	1	2
5_3	1) 0.03141	0.01	0.01	1.51E-05	3.38E-05	4.37E+02	6.40E+02
	2) 0.04806	0.02	0.02	2.43E-05	5.27E-05	3.52E+02	4.99E+02
		0.03	0.03	3.78E-05	8.03E-05	3.65E+02	5.07E+02
		0.04	0.04	5.17E-05	1.08E-04	3.74E+02	5.11E+02
		0.05	0.05	6.77E-05	1.36E-04	3.92E+02	5.13E+02
		0.06	0.06	1.08E-04	1.73E-04	5.21E+02	5.44E+02
		0.07	0.07	1.35E-04	2.00E-04	5.59E+02	5.41E+02
		0.08	0.08	1.54E-04	2.28E-04	5.59E+02	5.39E+02
		0.09	0.09	1.73E-04	2.56E-04	5.58E+02	5.37E+02
		0.1	0.1	1.92E-04	2.83E-04	5.55E+02	5.36E+02
		0.11	0.11	2.16E-04	3.20E-04	5.68E+02	5.51E+02
		0.12	0.12	2.35E-04	3.48E-04	5.67E+02	5.49E+02
		0.13	0.13	2.54E-04	3.76E-04	5.65E+02	5.47E+02
		0.14	0.14	2.72E-04	4.04E-04	5.63E+02	5.46E+02
		0.15	0.15	2.91E-04	4.31E-04	5.62E+02	5.44E+02
		0.16	0.16	3.17E-04	4.69E-04	5.73E+02	5.54E+02
		0.17	0.17	3.36E-04	4.96E-04	5.72E+02	5.53E+02
		0.18	0.18	3.55E-04	5.24E-04	5.71E+02	5.51E+02
		0.19	0.19	3.74E-04	5.52E-04	5.70E+02	5.50E+02
		0.20	0.20	3.94E-04	5.80E-04	5.70E+02	5.49E+02

Sample	Thickness (cm)	Applied Voltage (V)		Measured Current (A)		Conductivity (S/cm)	
		1	2	1	2	1	2
5_4	1) 0.03178	0.01	0.01	2.26E-05	3.43E-05	6.48E+02	7.58E+02
	2) 0.04119	0.02	0.02	3.66E-05	5.38E-05	5.23E+02	5.94E+02
		0.03	0.03	5.67E-05	8.27E-05	5.41E+02	6.09E+02
		0.04	0.04	7.71E-05	1.11E-04	5.52E+02	6.15E+02
		0.05	0.05	9.78E-05	1.40E-04	5.60E+02	6.17E+02
		0.06	0.06	1.25E-04	1.78E-04	5.95E+02	6.54E+02
		0.07	0.07	1.45E-04	2.06E-04	5.94E+02	6.50E+02
		0.08	0.08	1.66E-04	2.35E-04	5.94E+02	6.47E+02
		0.09	0.09	1.87E-04	2.63E-04	5.94E+02	6.45E+02
		0.1	0.1	2.07E-04	2.91E-04	5.93E+02	6.44E+02
		0.11	0.11	2.34E-04	3.29E-04	6.10E+02	6.60E+02
		0.12	0.12	2.56E-04	3.57E-04	6.11E+02	6.57E+02
		0.13	0.13	2.78E-04	3.85E-04	6.11E+02	6.55E+02
		0.14	0.14	2.99E-04	4.14E-04	6.11E+02	6.52E+02
		0.15	0.15	3.21E-04	4.42E-04	6.12E+02	6.50E+02
		0.16	0.16	3.50E-04	4.79E-04	5.26E+02	6.62E+02

Sample	Thickness (cm)	Applied Voltage (V)		Measured Current (A)		Conductivity (S/cm)	
		1	2	1	2	1	2
5_4	1) 0.03178	0.17	0.17	3.71E-04	5.07E-04	5.25E+02	6.59E+02
	2) 0.04119	0.18	0.18	3.94E-04	5.35E-04	5.27E+02	6.57E+02
		0.19	0.19	4.17E-04	5.64E-04	5.28E+02	6.55E+02
		0.20	0.20	4.39E-04	5.92E-04	5.29E+02	6.53E+02

Sample	Thickness (cm)	Applied Voltage (V)		Measured Current (A)		Conductivity (S/cm)	
		1	2	1	2	1	2
5_5	1) 0.02844	0.01	0.01	2.18E-05	2.45E-05	6.98E+02	7.34E+02
	2) 0.03037	0.02	0.02	3.39E-05	3.66E-05	5.43E+02	5.48E+02
		0.03	0.03	5.18E-05	5.54E-05	5.53E+02	5.53E+02
		0.04	0.04	6.96E-05	7.40E-05	5.56E+02	5.54E+02
		0.05	0.05	8.72E-05	9.24E-05	5.58E+02	5.54E+02
		0.06	0.06	1.11E-04	1.17E-04	5.92E+02	5.85E+02
		0.07	0.07	1.29E-04	1.36E-04	5.88E+02	5.80E+02
		0.08	0.08	1.46E-04	1.54E-04	5.84E+02	5.77E+02
		0.09	0.09	1.64E-04	1.72E-04	5.83E+02	5.74E+02
		0.1	0.1	1.83E-04	1.90E-04	5.84E+02	5.69E+02
		0.11	0.11	2.06E-04	2.15E-04	5.98E+02	5.85E+02
		0.12	0.12	2.23E-04	2.33E-04	5.94E+02	5.81E+02
		0.13	0.13	2.41E-04	2.51E-04	5.93E+02	5.78E+02
		0.14	0.14	2.58E-04	2.69E-04	5.90E+02	5.75E+02
		0.15	0.15	2.76E-04	2.87E-04	5.88E+02	5.73E+02
		0.16	0.16	3.00E-04	3.11E-04	6.01E+02	5.83E+02
		0.17	0.17	3.18E-04	3.30E-04	5.98E+02	5.81E+02
		0.18	0.18	3.36E-04	3.48E-04	5.96E+02	5.78E+02
		0.19	0.19	3.55E-04	3.65E-04	5.97E+02	5.75E+02
		0.20	0.20	3.74E-04	3.83E-04	5.98E+02	5.74E+02

Appendix G: Electrorheological Properties Measurement of pure PDMS and PDMS_PEDOT/PSS blend

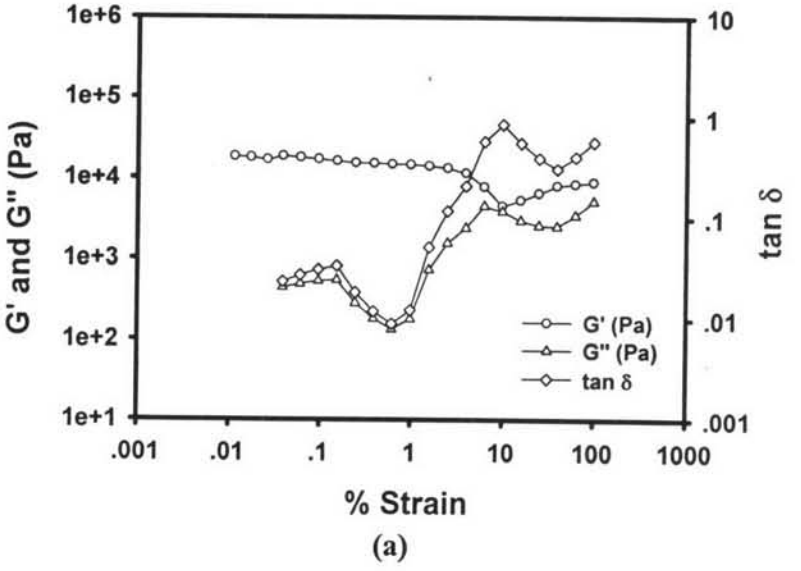

(a)

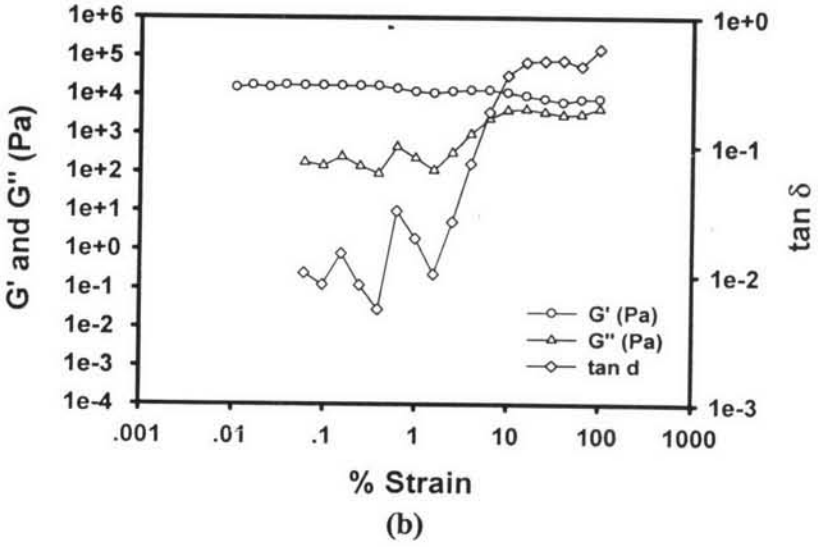

(b)

Figure G1 Strain sweep test of pure PDMS, frequency 1.0 rad/s, 27 °C, gap 0.820 mm at: (a) E=0 V/mm; (b) E=2000 V/mm.

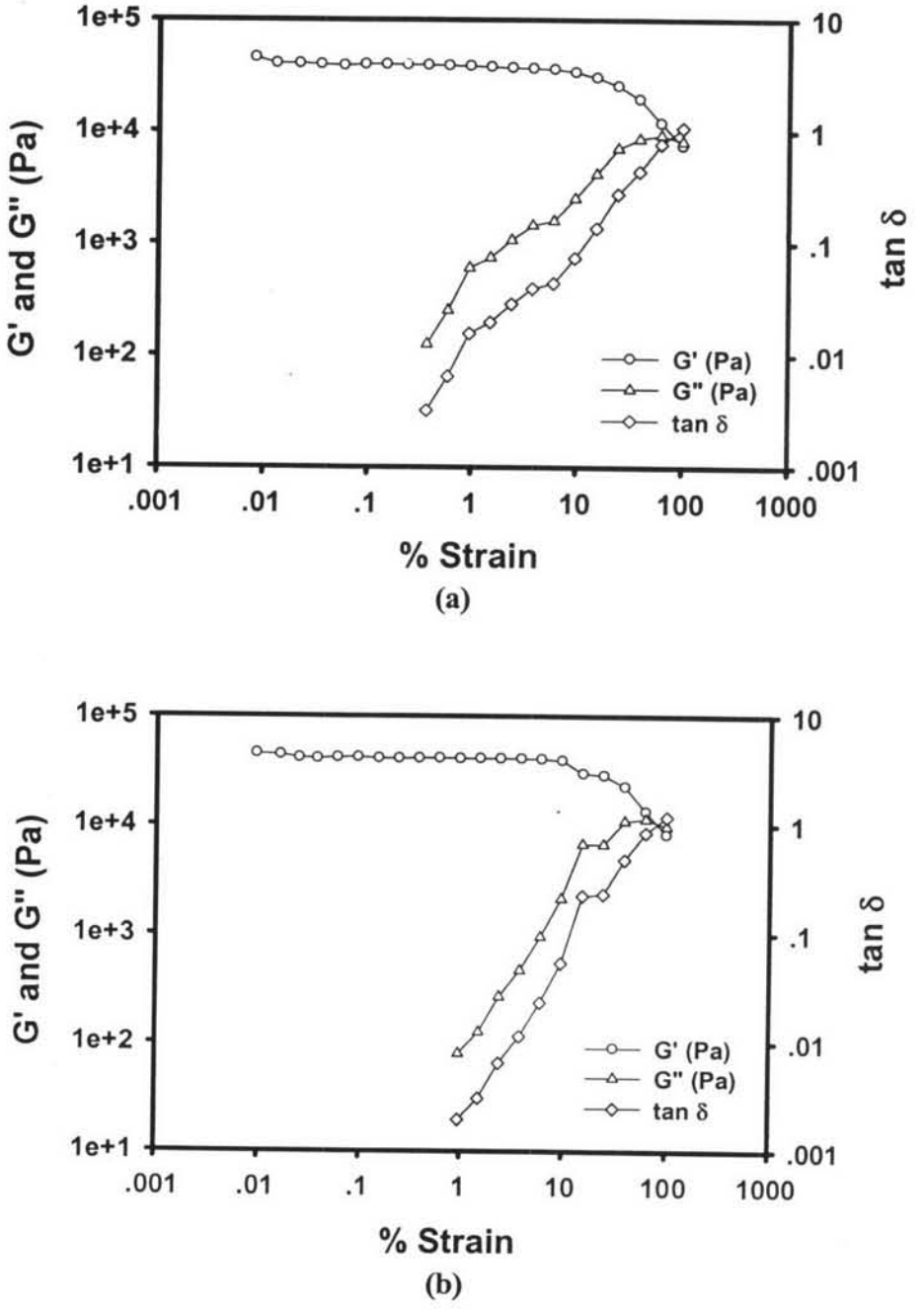

Figure G2 Strain sweep test of PDMS_5%PEDOT/PSS, frequency 1.0 rad/s, 27 °C, gap 0.670 mm at: (a) E=0 V/mm; (b) E=2000 V/mm.

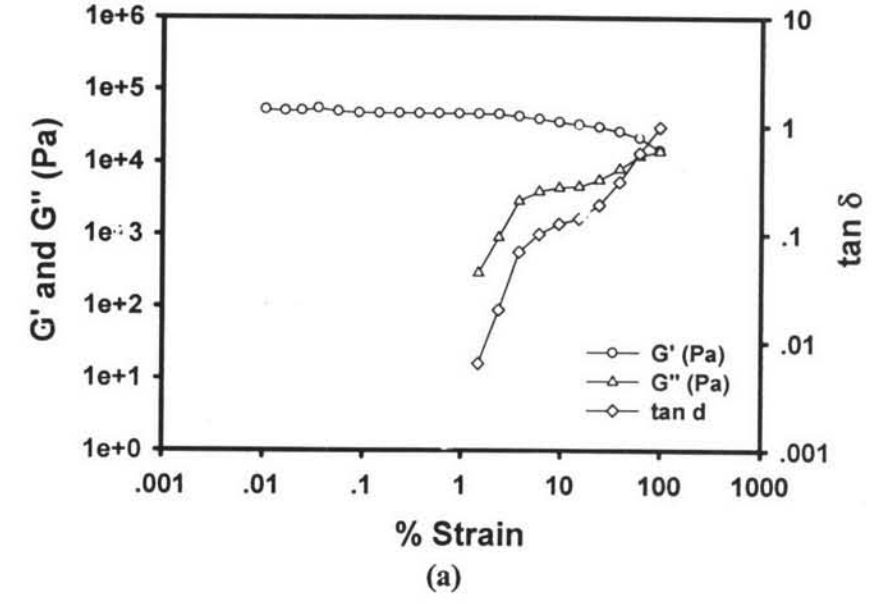

(a)

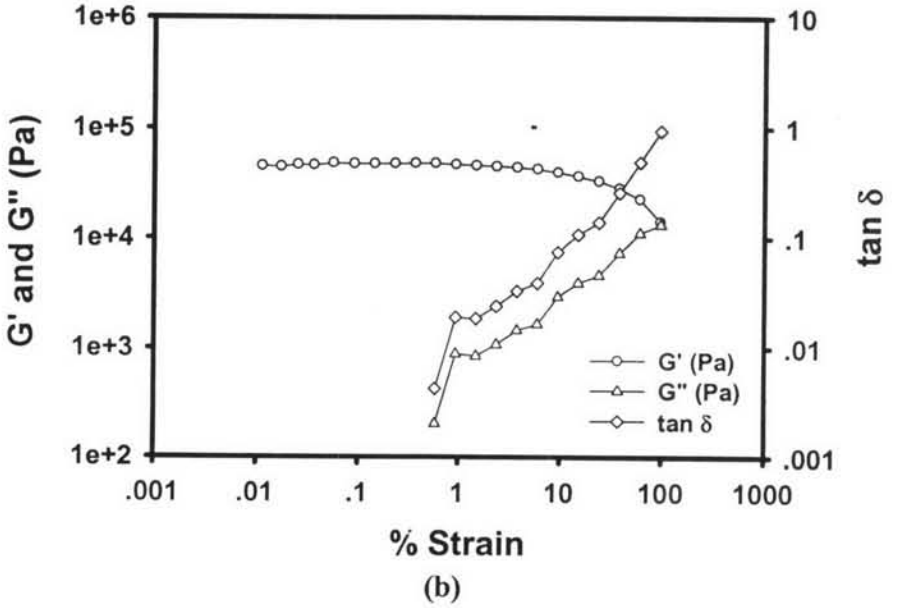

(b)

Figure G3 Strain sweep test of PDMS_10%PEDOT/PSS, frequency 1.0 rad/s, 27 °C, gap 0.630 mm at: (a) E=0 V/mm; (b) E=2000 V/mm.

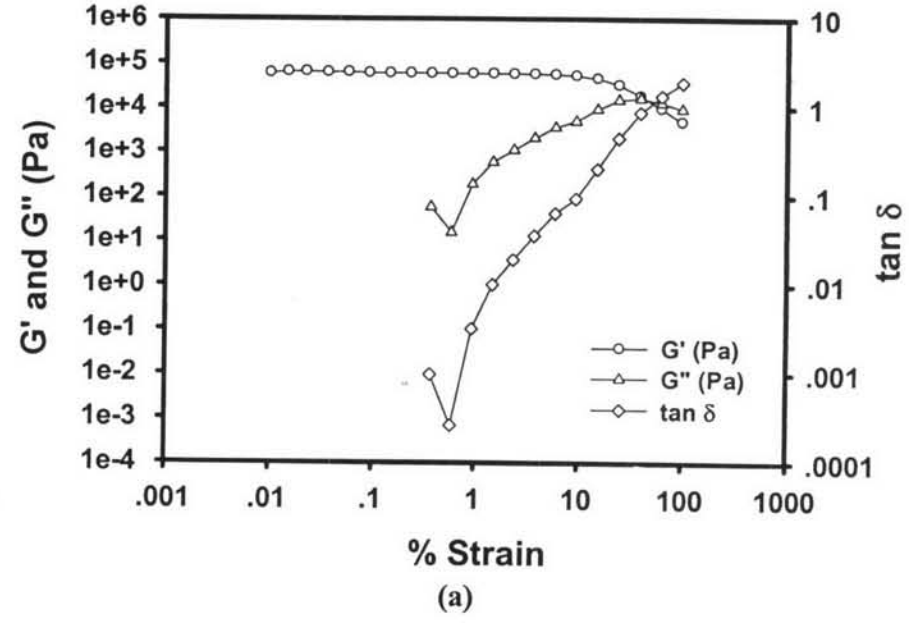

(a)

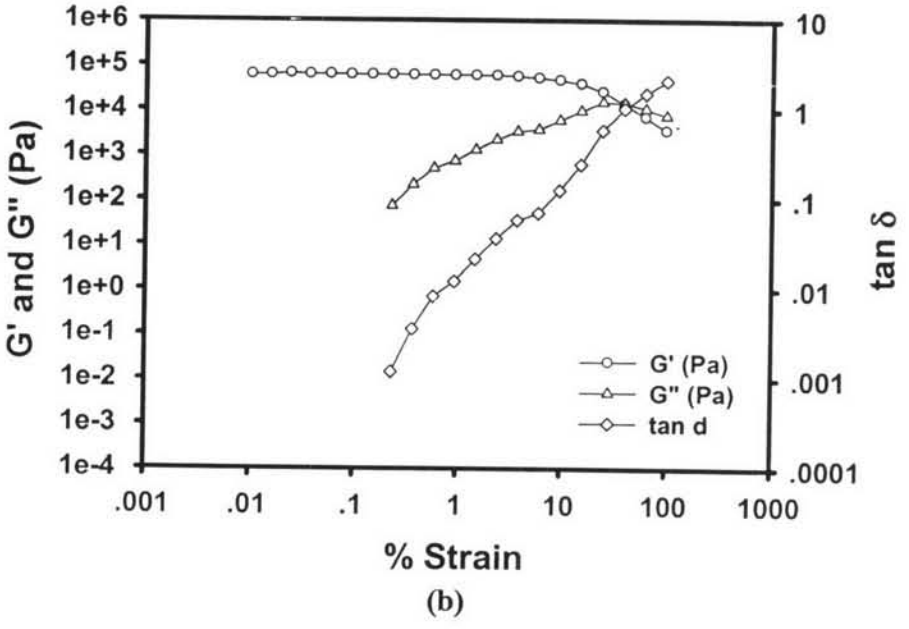

(b)

Figure G4 Strain sweep test of PDMS_15%PEDOT/PSS, frequency 1.0 rad/s, 27 °C, gap 0.780 mm at: (a) E=0 V/mm; (b) E=2000 V/mm.

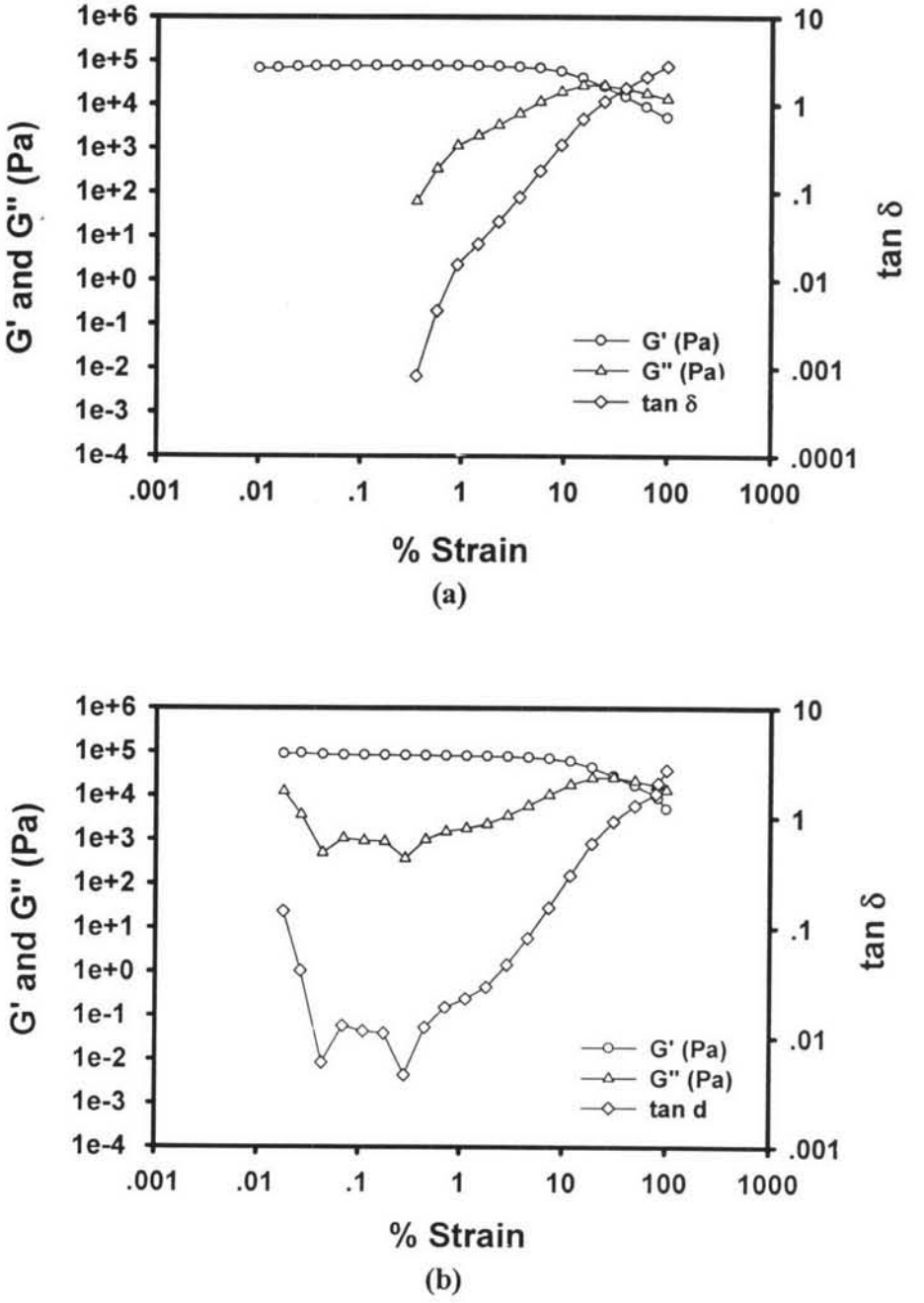

Figure G5 Strain sweep test of PDMS_20%PEDOT/PSS, frequency 1.0 rad/s, 27 °C, gap 0.620 mm at: (a) E=0 V/mm; (b) E=2000 V/mm.

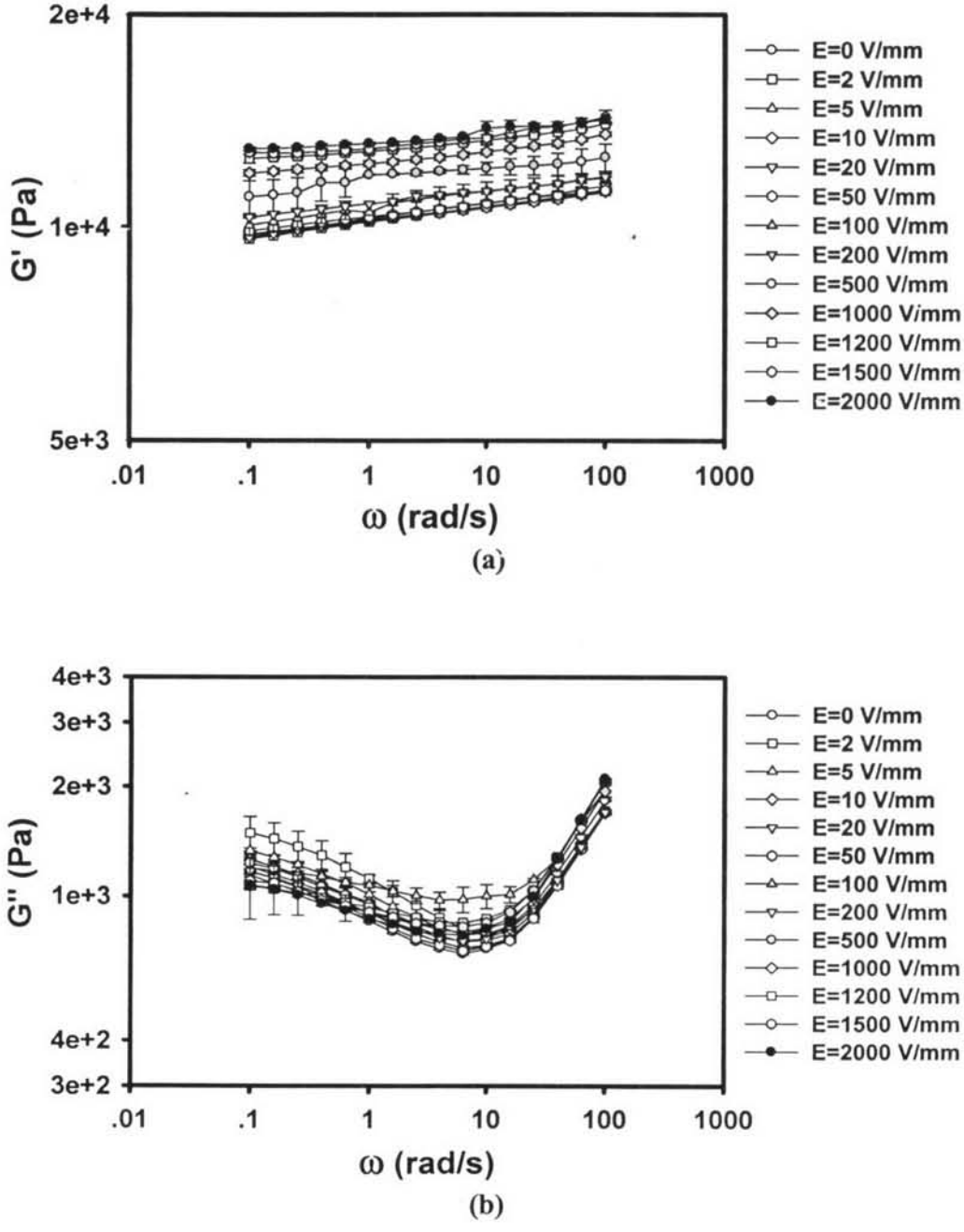

Figure G6 Storage and loss moduli of pure PDMS at various electric field strengths vs. frequency, strain 3.0%, 27 °C, gap 0.820 mm,: (a) storage modulus, G'(ω); (b) loss modulus, G"(ω).

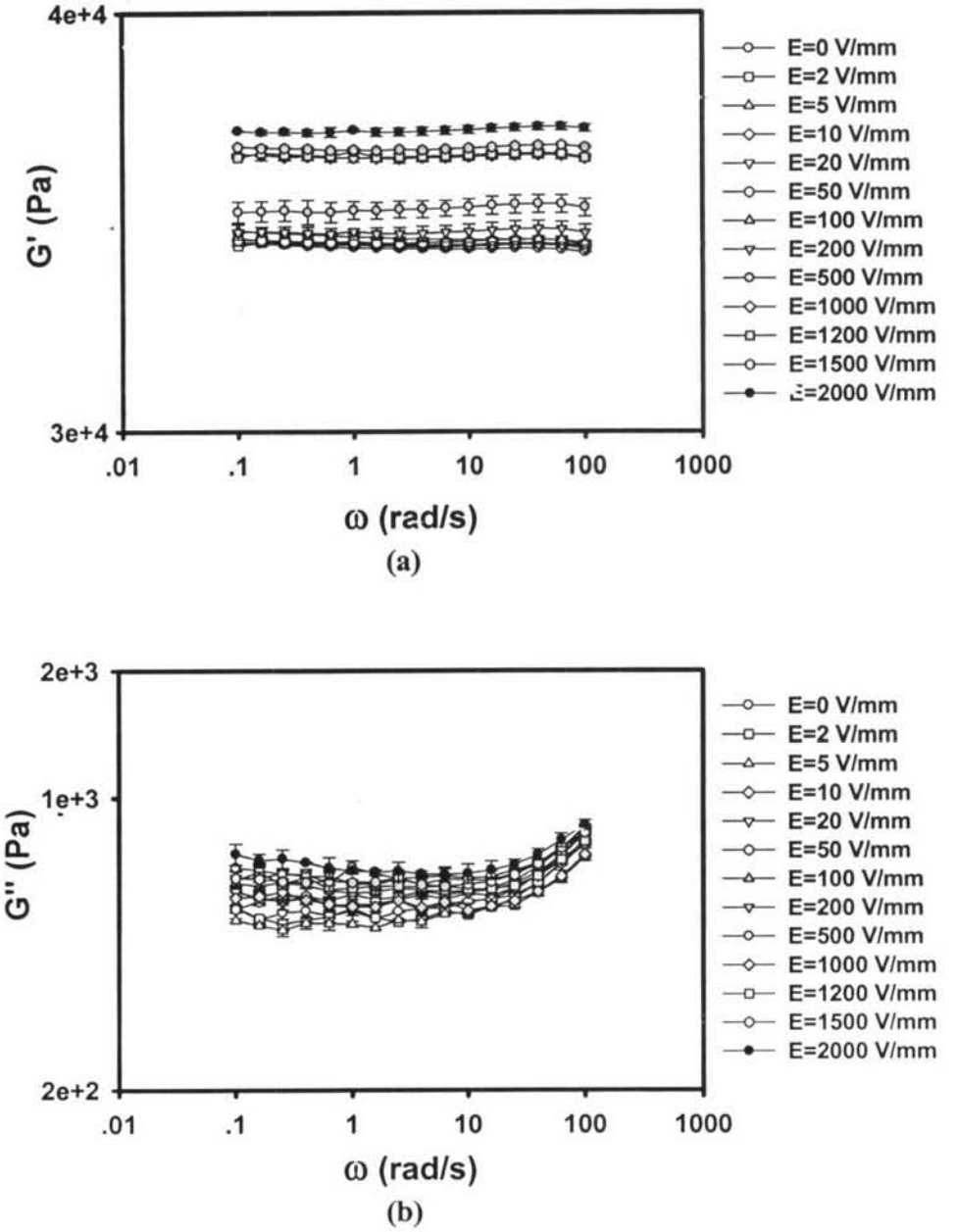

Figure G7 Storage and loss moduli of PDMS_5%PEDOT/PSS at various electric field strengths vs. frequency, strain 3.0%, 27 °C, gap 0.670 mm,: (a) storage modulus, G'(ω); (b) loss modulus, G"(ω).

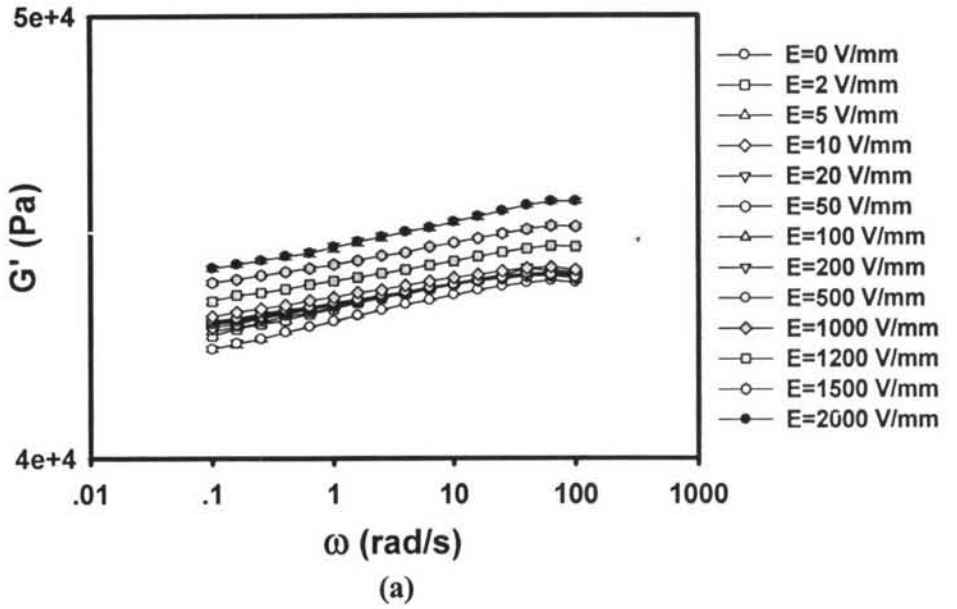

(a)

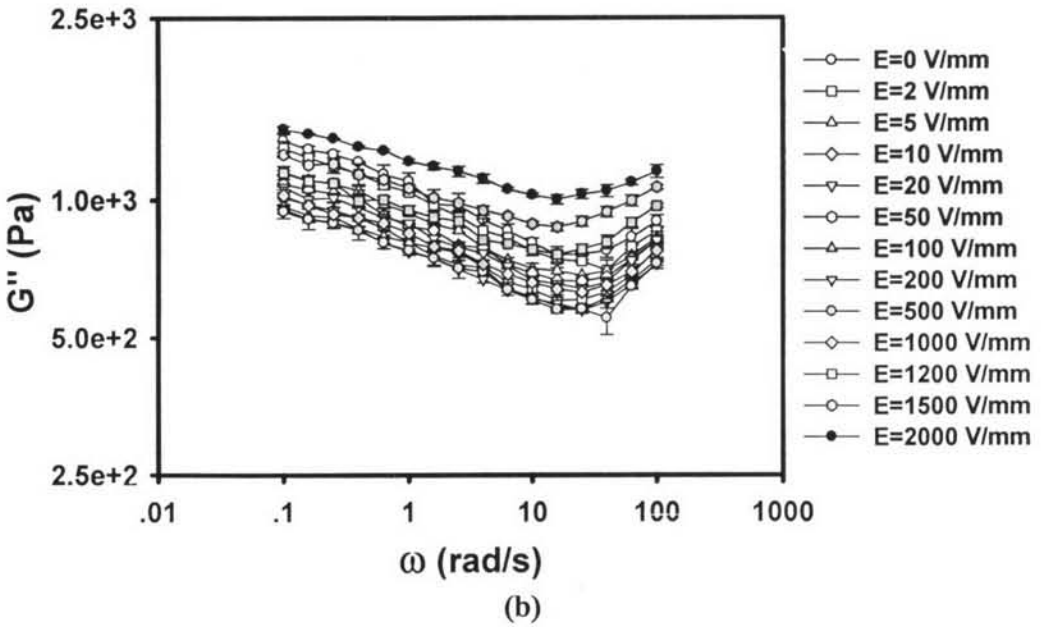

(b)

Figure G8 Storage and loss moduli of PDMS_10%PEDOT/PSS at various electric field strengths vs. frequency, strain 3.0%, 27 °C, gap 0.630 mm,: (a) storage modulus, G'(ω); (b) loss modulus, G"(ω).

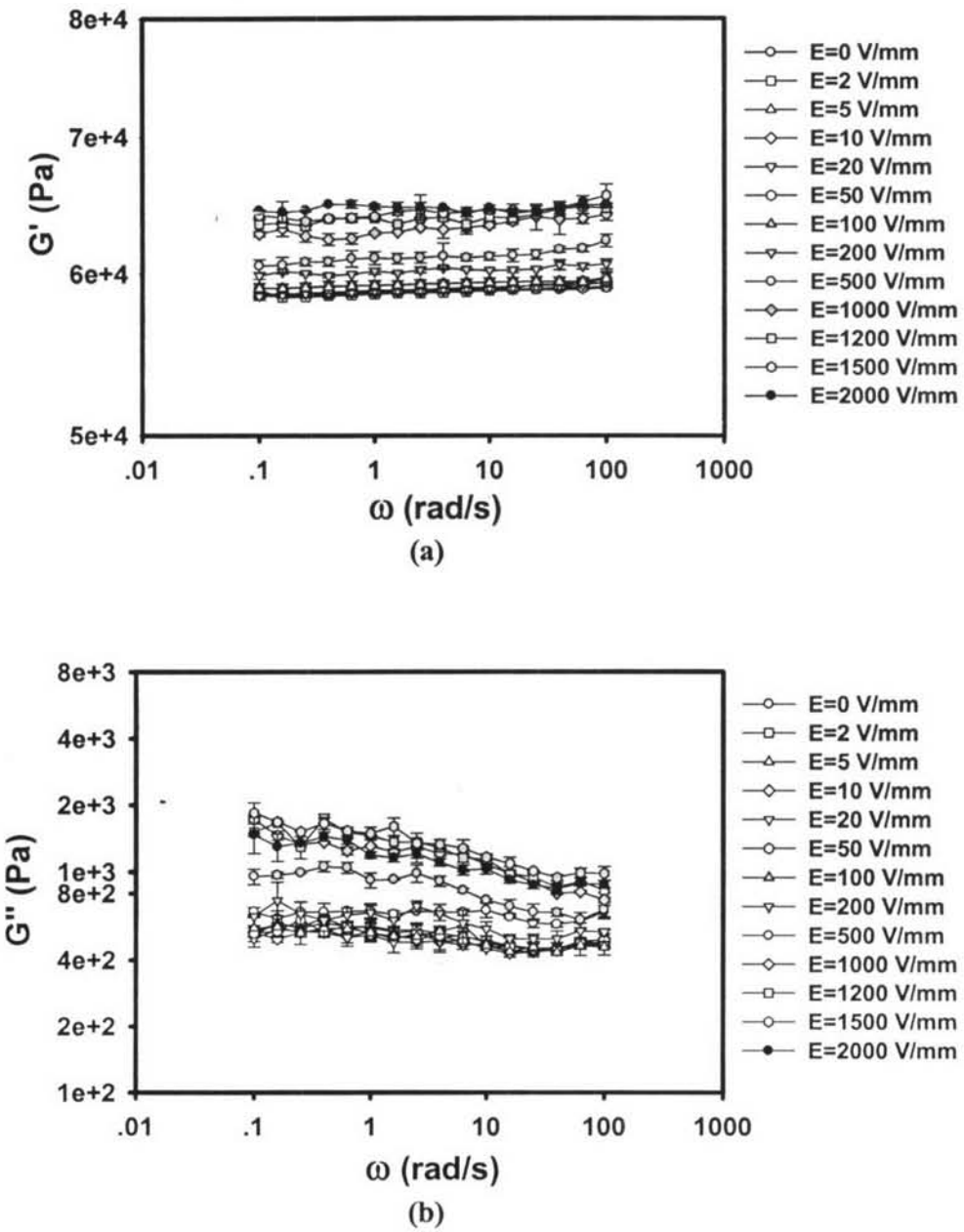

Figure G9 Storage and loss moduli of PDMS_15%PEDOT/PSS at various electric field strengths vs. frequency, strain 3.0%, 27 °C, gap 0.780 mm,: (a) storage modulus, G'(ω); (b) loss modulus, G"(ω).

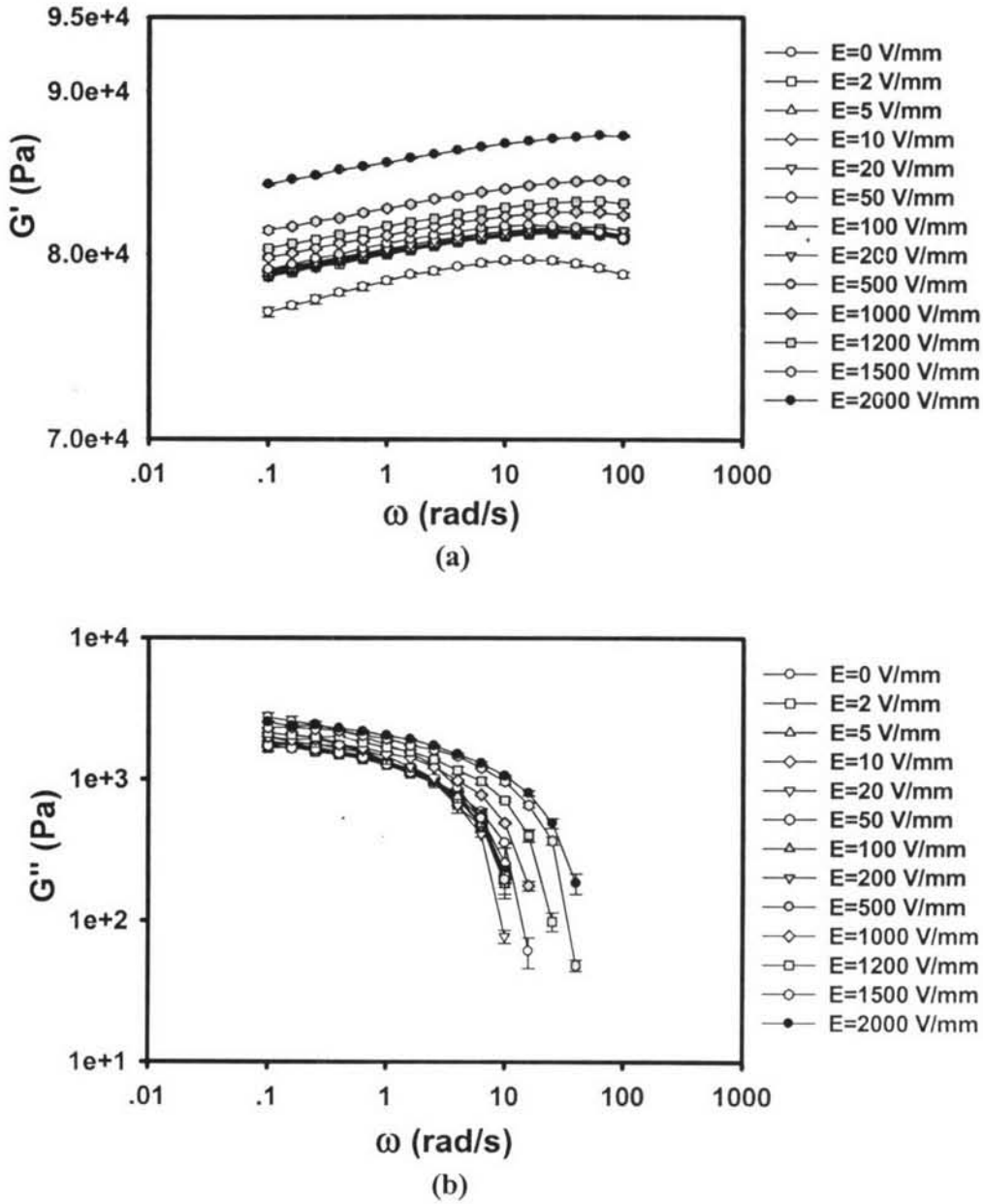

Figure G10 Storage and loss moduli of PDMS_20%PEDOT/PSS at various electric field strengths vs. frequency, strain 3.0%, 27 °C, gap 0.620 mm,: (a) storage modulus, G'(ω); (b) loss modulus, G"(ω).

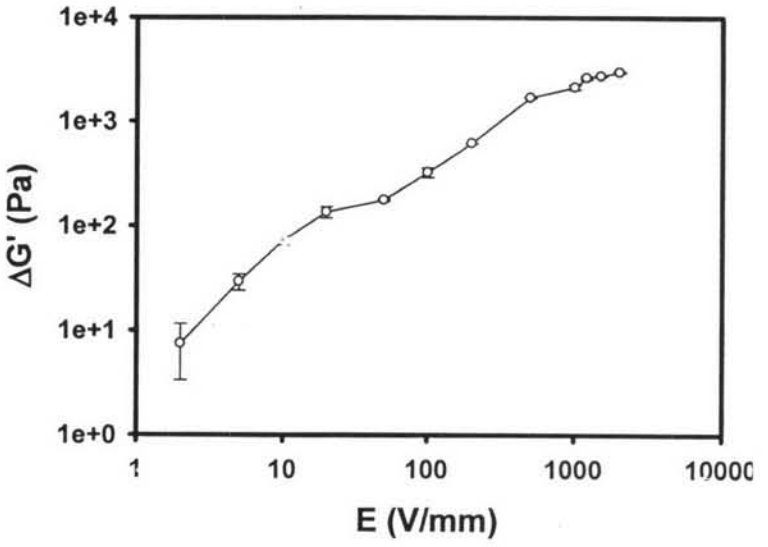

Figure G11 The storage modulus response (ΔG') of pure PDMS vs. electric field strength at frequency 1.0 rad/s, strain 3.0%, 27°C, gap 0.820 mm when $G'_0 = 10167$ Pa.

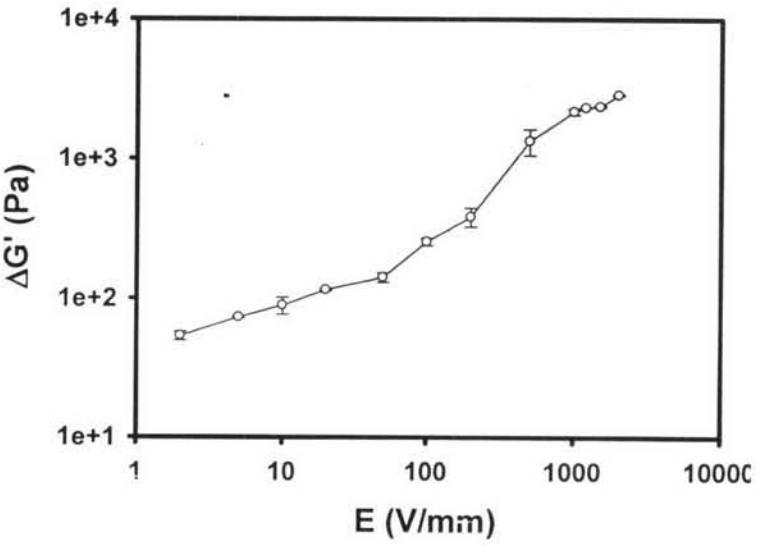

Figure G12 The storage modulus response (ΔG') of PDMS_5%PEDOT/PSS vs. electric field strength at frequency 1.0 rad/s, strain 3.0%, 27°C, gap 0.670 mm when $G'_0 = 34032$ Pa.

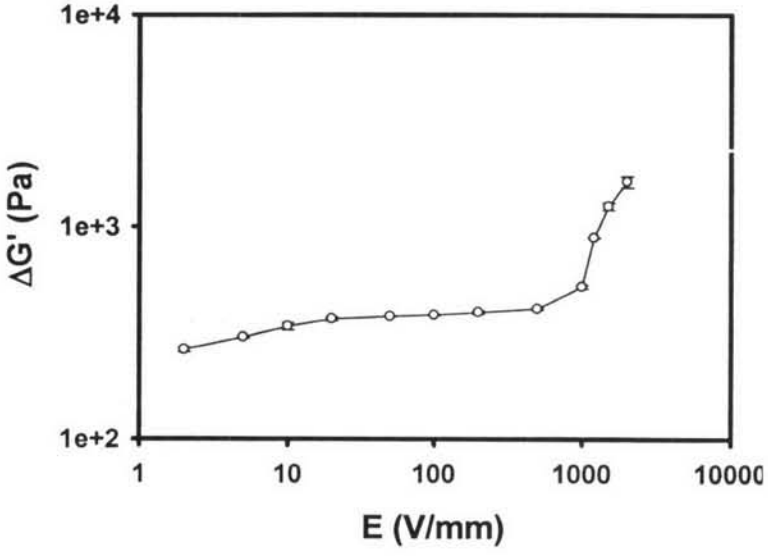

Figure G13 The storage modulus response (ΔG') of PDMS_10%PEDOT/PSS vs. electric field strength at frequency 1.0 rad/s, strain 3.0%, 27°C, gap 0.630 mm when G'_0 = 42861 Pa.

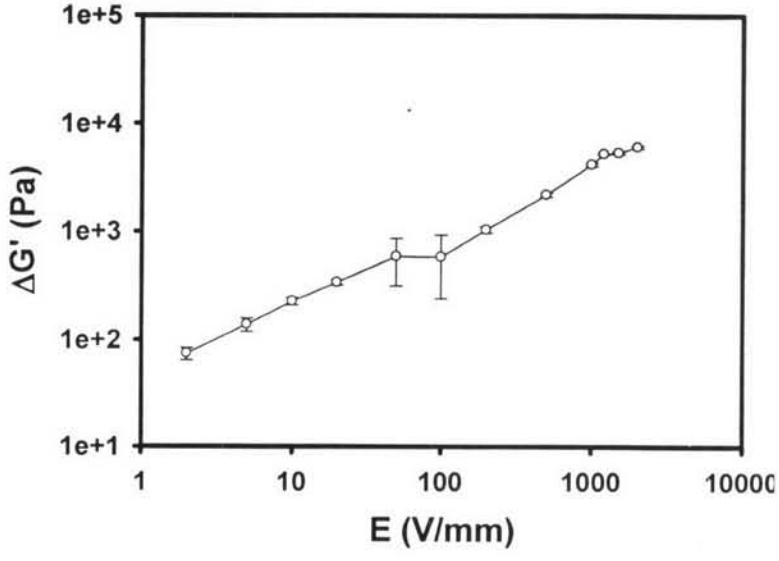

Figure G14 The storage modulus response (ΔG') of PDMS_15%PEDOT/PSS vs. electric field strength at frequency 1.0 rad/s, strain 3.0%, 27°C, gap 0.780 mm when G'_0 = 58650 Pa.

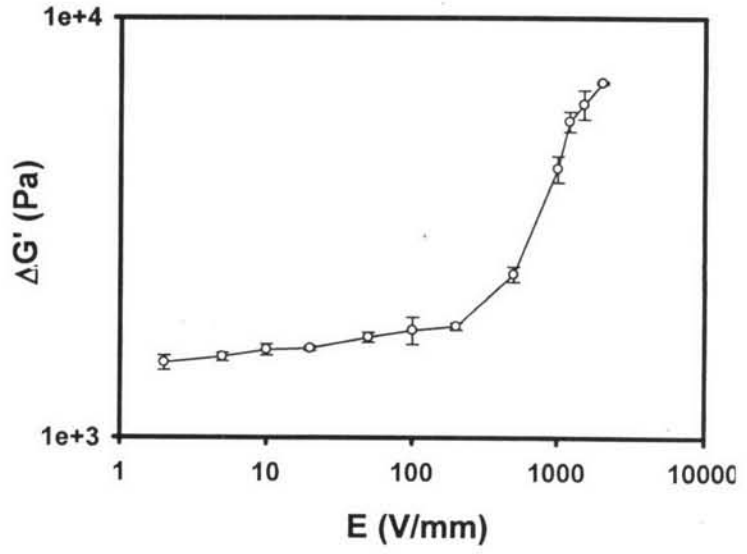

Figure G15 The storage modulus response (ΔG') of PDMS_20%PEDOT/PSS vs. electric field strength at frequency 1.0 rad/s, strain 3.0%, 27°C, gap 0.620 mm when G'_0 = 78486 Pa.

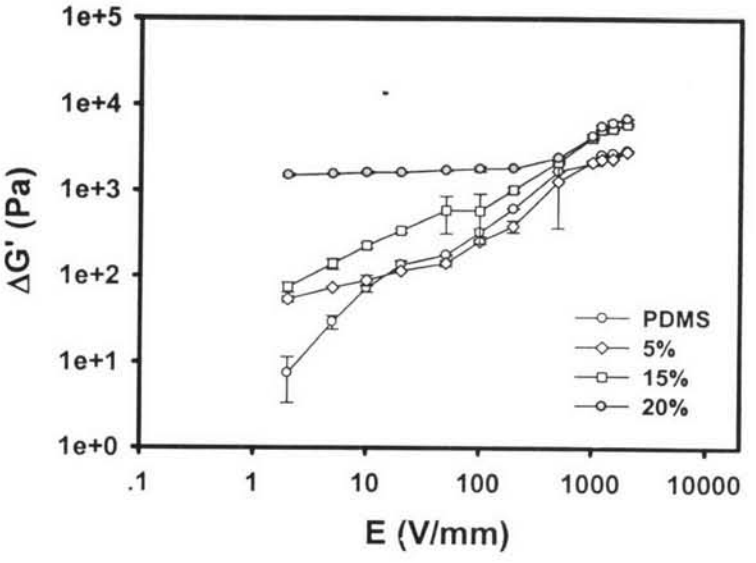

Figure G16 The storage modulus response (ΔG') of pure PDMS and PDMS_PEDOT/PSS blends at various particle concentrations vs. electric field strength at frequency 1.0 rad/s, strain 3.0% and at 27°C.

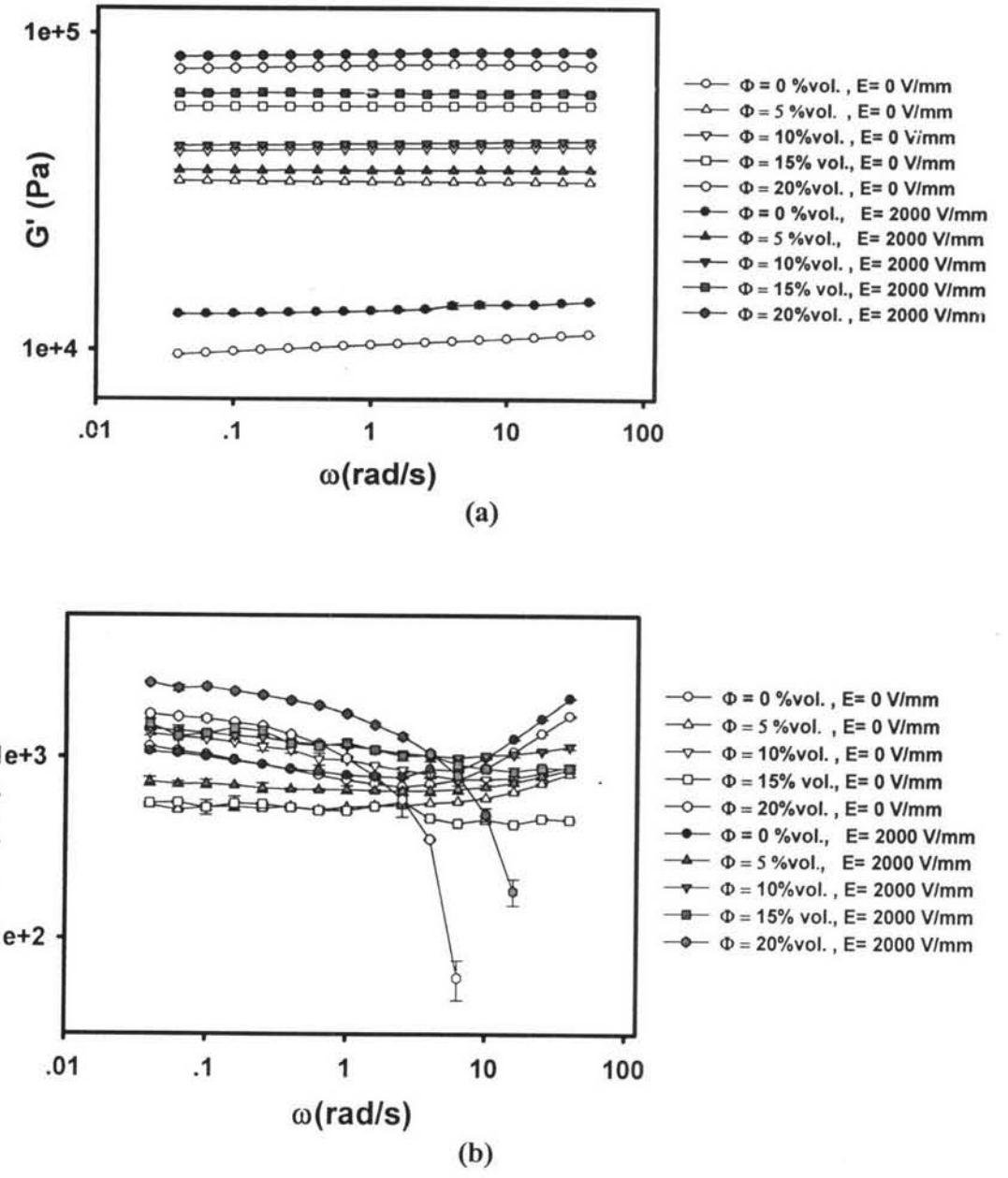

Figure G17 Comparison of the storage modulus of pure PDMS (Φ = 0 %vol.) and PDMS_PEDOT/PSS blends at various particle concentrations (Φ = 5, 10, 15, and 20 %vol.) vs. frequency, strain 3.0%, 27°C at electric field strengths of 0 and 2 kV/mm: (a) storage modulus, G'(ω); (b) loss modulus, G"(ω).

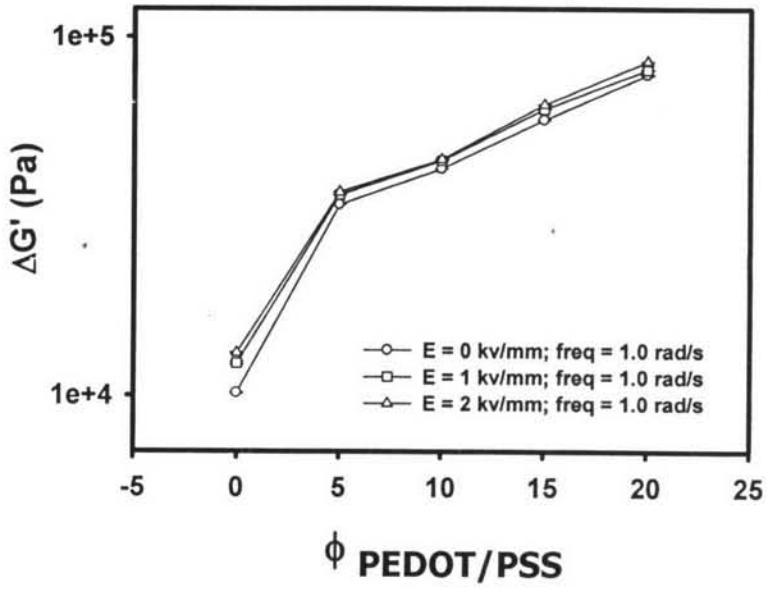

Figure G18 Comparison of the storage modulus response (ΔG') of pure PDMS and PDMS_PEDOT/PSS blends at various electric field strengths (0, 1 and 2 kV/mm) vs. particle concentrations (Φ = 0, 5, 10, 15, and 20 %vol.), frequency 1.0 rad/s, strain 3.0% and at 27°C.

Appendix H: Electrorheological Properties Measurement of PDMS_PEDOT/PSS/ EG blend

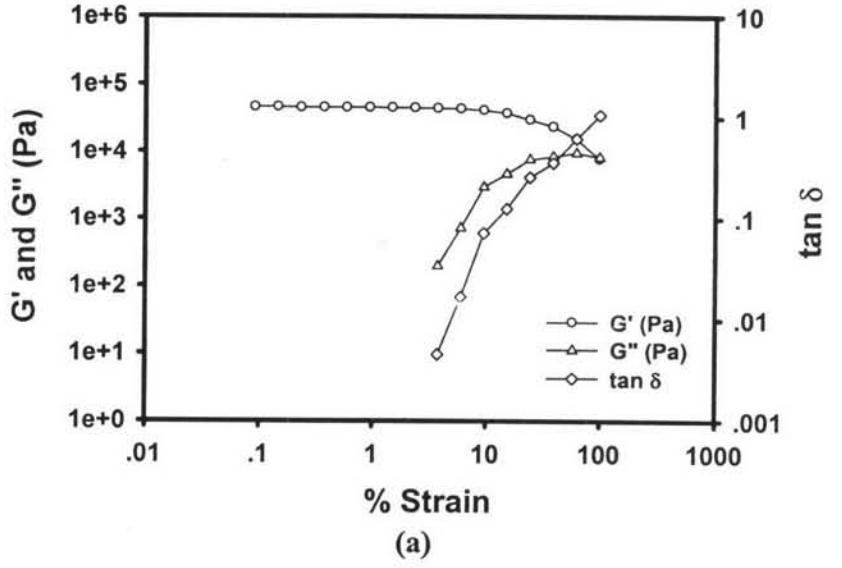

(a)

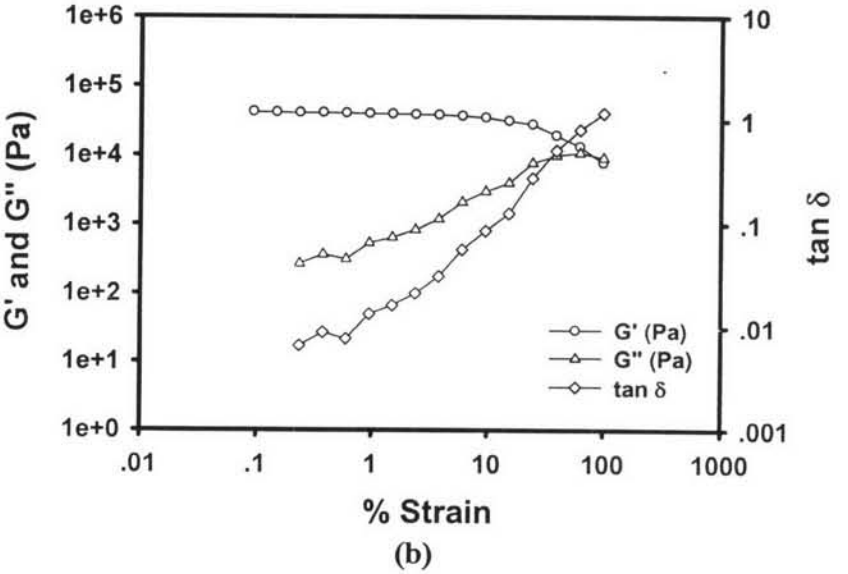

(b)

Figure H1 Strain sweep test of PDMS_5%PEDOT/PSS/EG, frequency 1.0 rad/s, 27 °C, gap 0.850 mm at: (a) E=0 V/mm; (b) E=2000 V/mm.

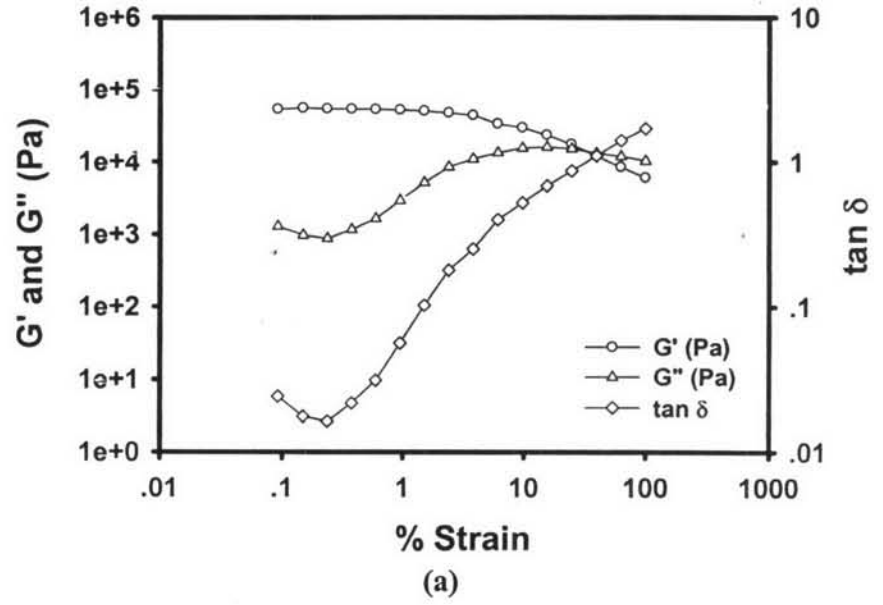

(a)

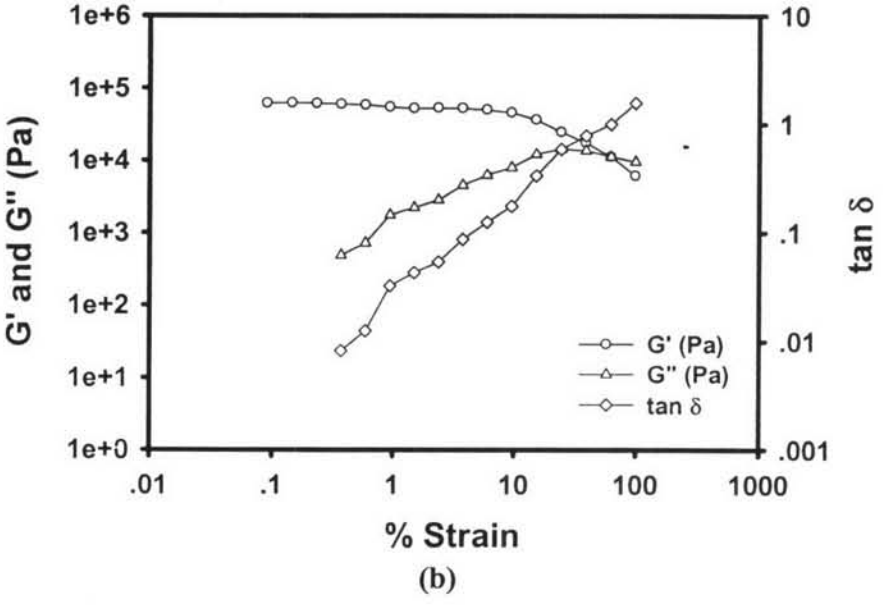

(b)

Figure H2 Strain sweep test of PDMS_10%PEDOT/PSS/EG, frequency 1.0 rad/s, 27 °C, gap 0.770 mm at: (a) E=0 V/mm; (b) E=2000 V/mm.

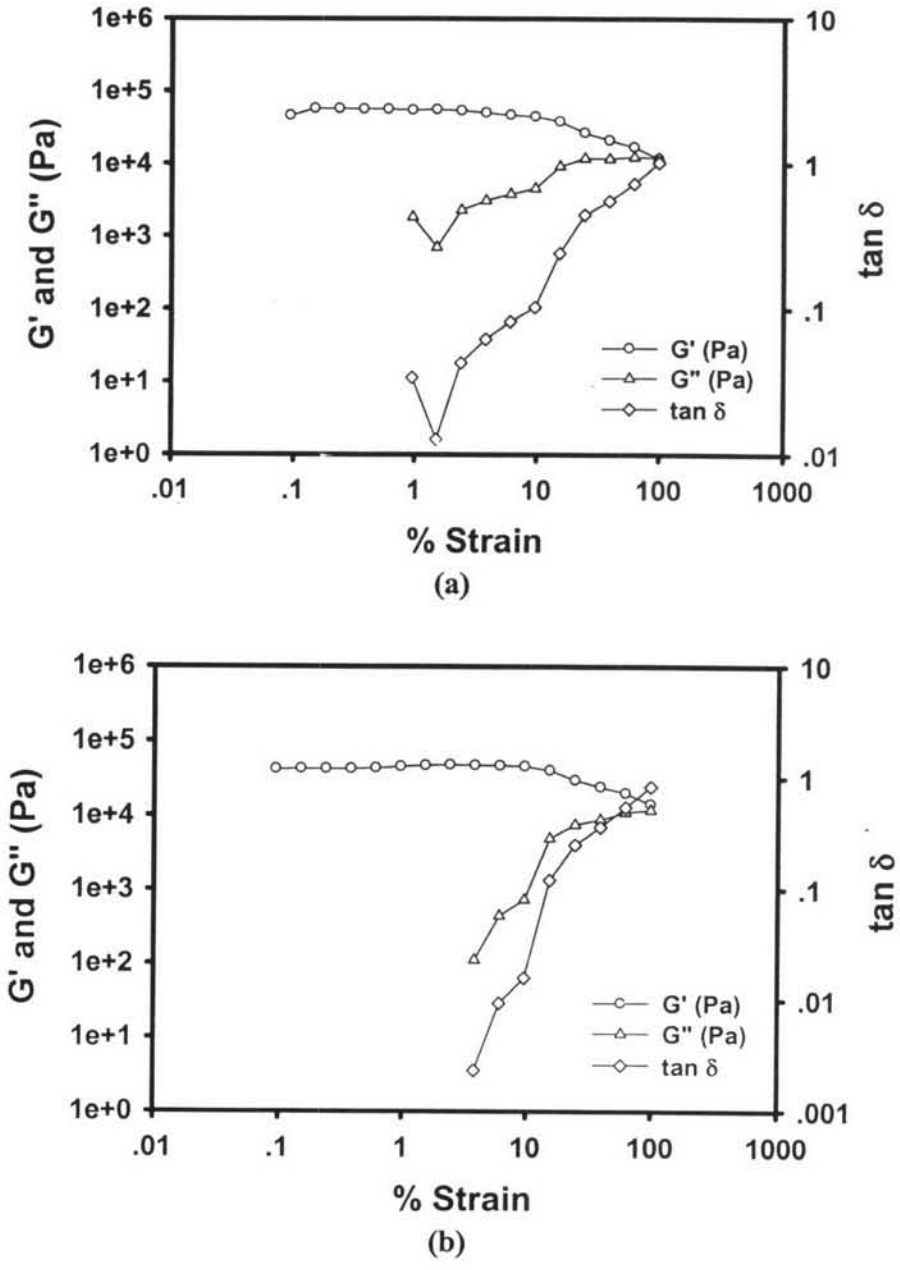

Figure H3 Strain sweep test of PDMS_15%PEDOT/PSS/EG, frequency 1.0 rad/s, 27 °C, gap 0.830 mm at: (a) E=0 V/mm; (b) E=2000 V/mm.

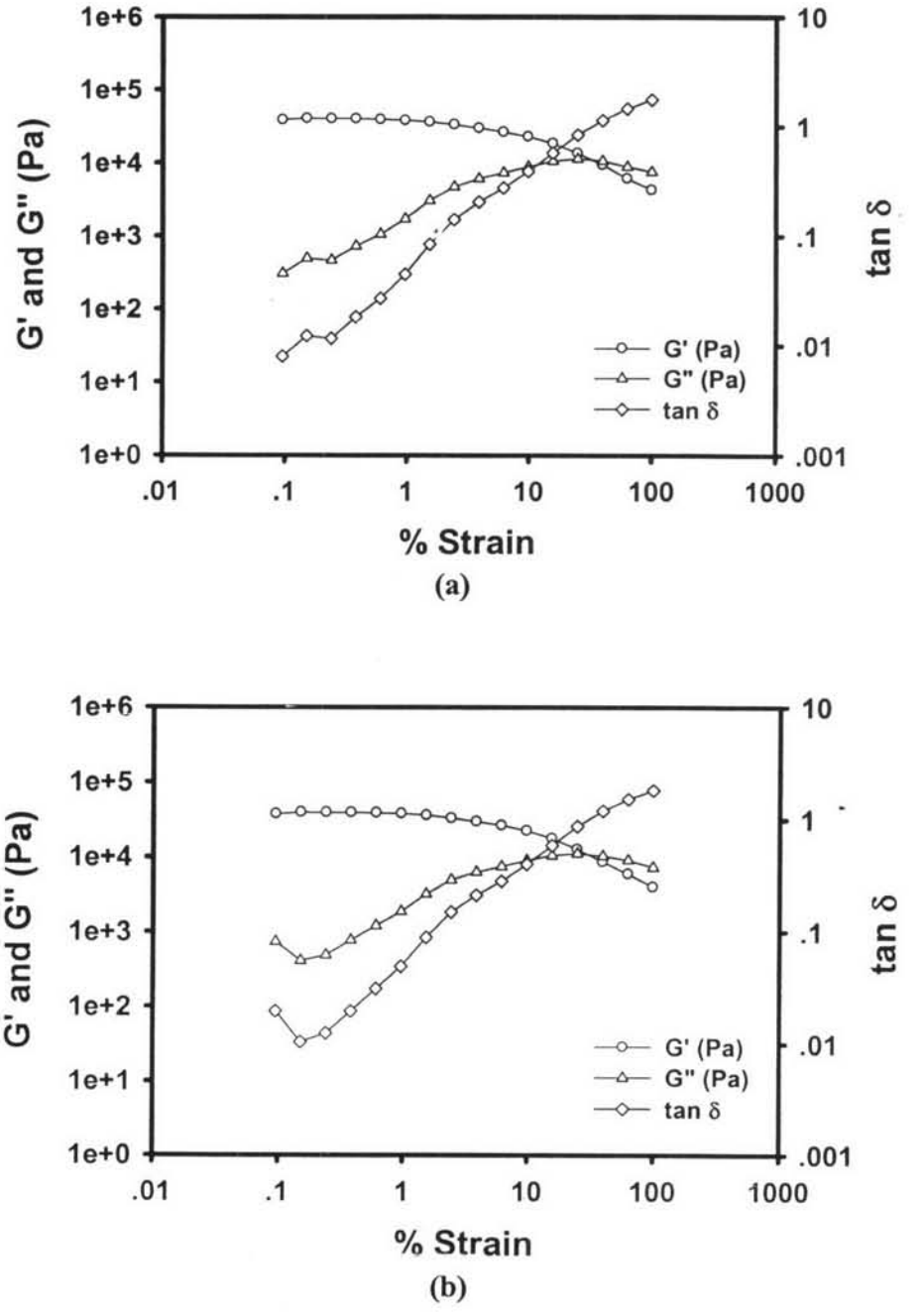

Figure H4 Strain sweep test of PDMS_20%PEDOT/PSS/EG, frequency 1.0 rad/s, 27 °C, gap 0.780 mm at: (a) E=0 V/mm; (b) E=300 V/mm.

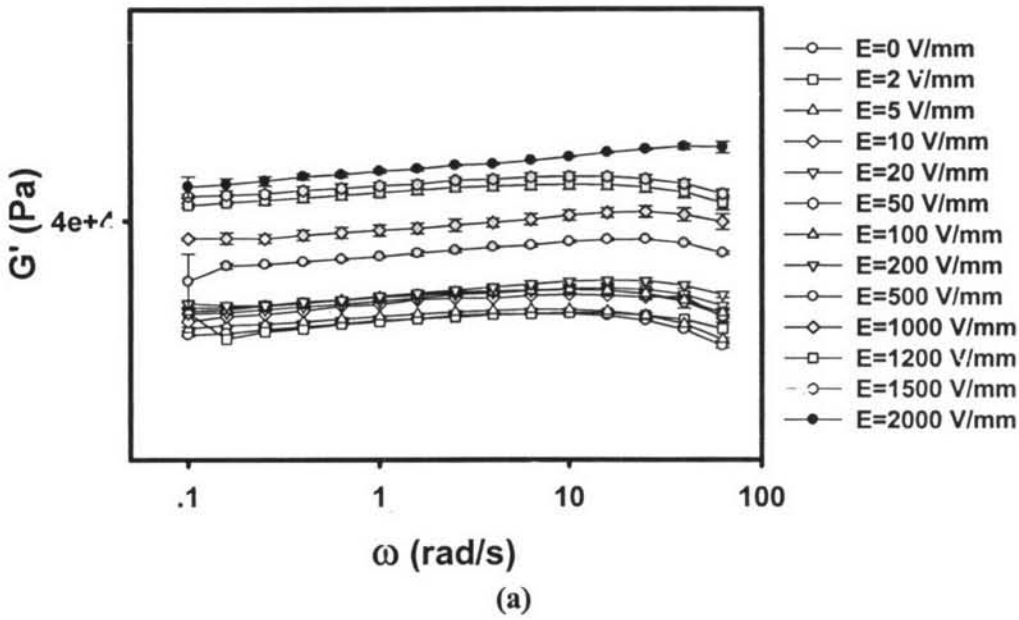

(a)

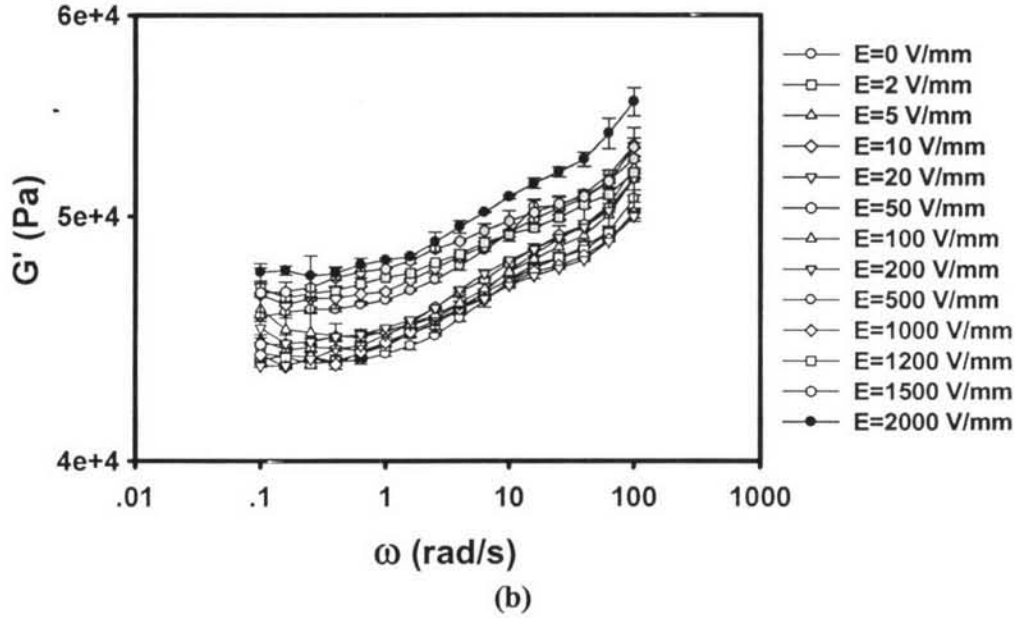

(b)

Figure H5 Storage modulus of: (a) PDMS_5%PEDOT/PSS/EG, (b) PDMS_10% PEDOT/PSS/EG at various electric field strengths vs. frequency, strain 3.0%, 27 °C, gap 0.800 mm and 0.830 mm, respectively.

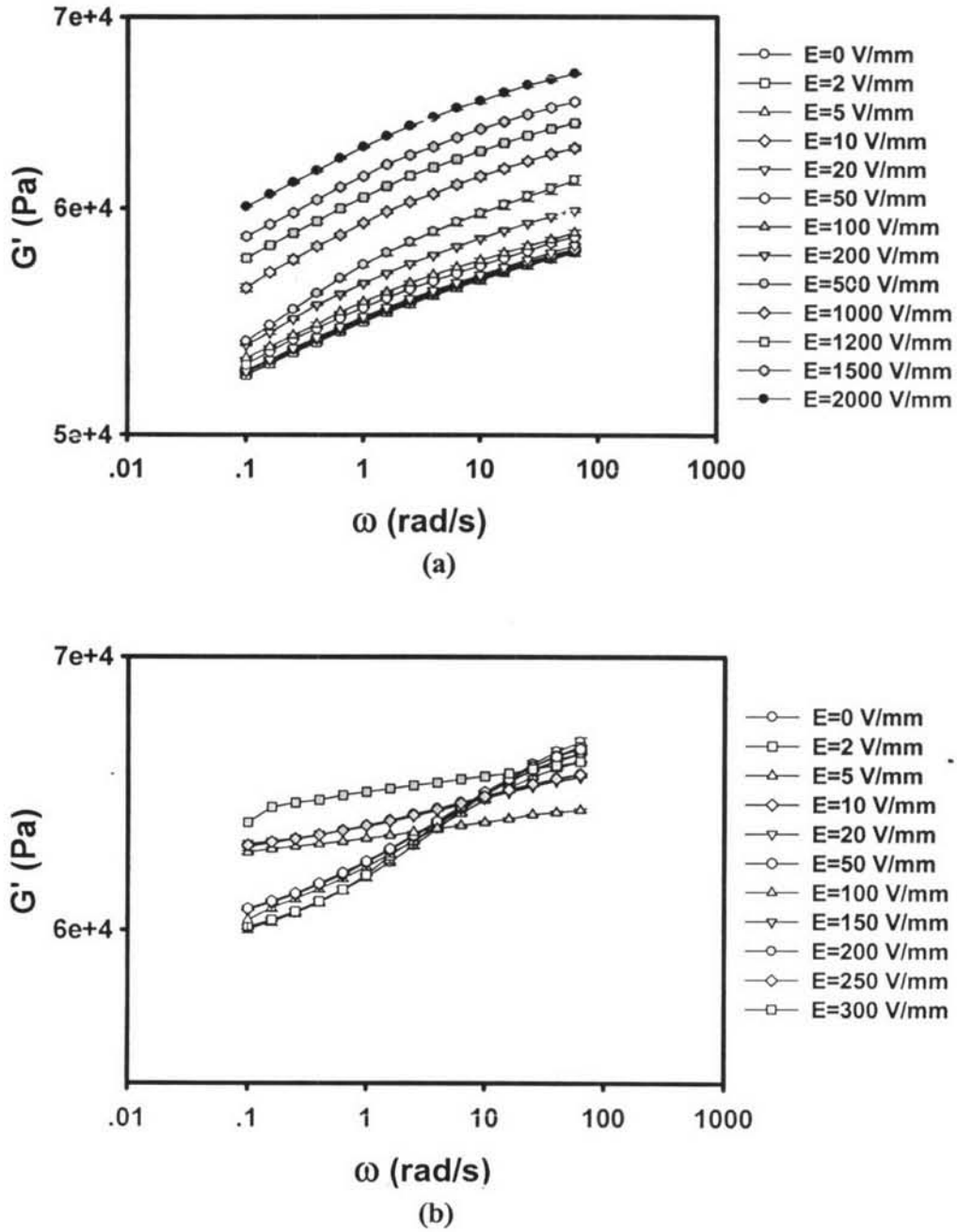

Figure H6 Storage modulus of: (a) PDMS_15%PEDOT/PSS/EG, (b) PDMS_20% PEDOT/PSS/EG at various electric field strengths vs. frequency, strain 3.0%, 27 °C, gap 0.815 mm and 0.820 mm, respectively.

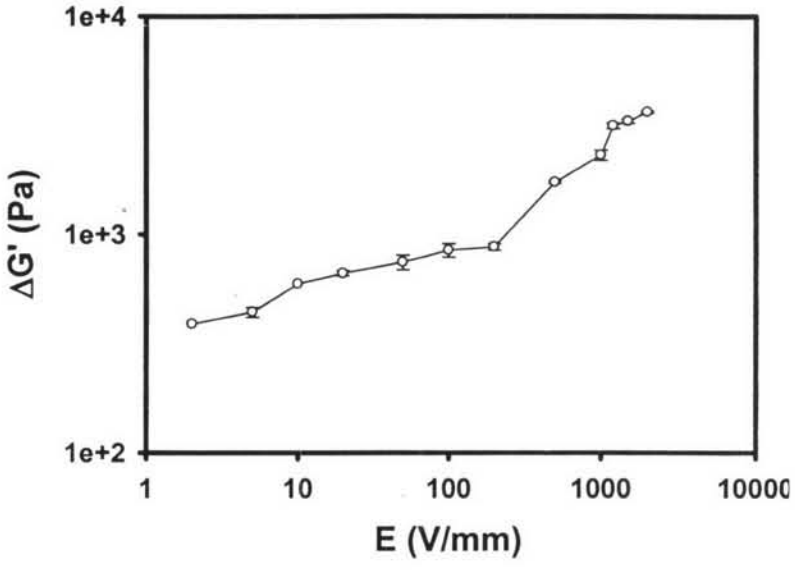

Figure H7 The storage modulus response (ΔG') of PDMS_5%PEDOT/PSS/EG vs. electric field strength at frequency 1.0 rad/s, strain 3.0%, 27°C, gap 0.760 mm when G'_0 = 10167 Pa.

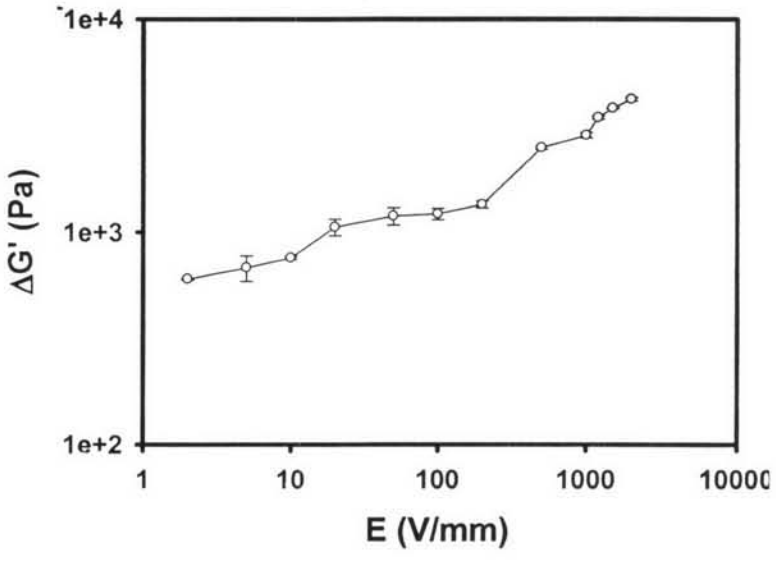

Figure H8 The storage modulus response (ΔG') of PDMS_10%PEDOT/PSS/EG vs. electric field strength at frequency 1.0 rad/s, strain 3.0%, 27°C, gap 0.870 mm when G'_0 = 37835 Pa.

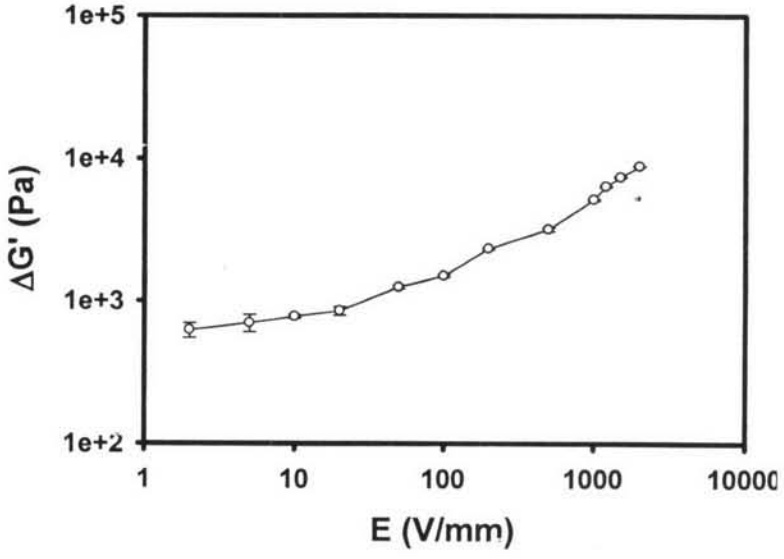

Figure H9 The storage modulus response (ΔG') of PDMS_15%PEDOT/PSS/EG vs. electric field strength at frequency 1.0 rad/s, strain 3.0%, 27°C, gap 0.730 mm when G'_0 = 44130 Pa.

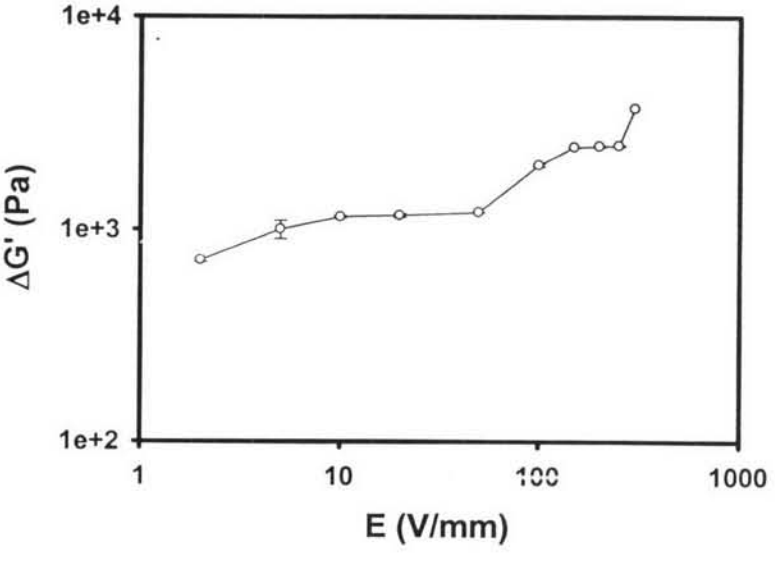

Figure H10 The storage modulus response (ΔG') of PDMS_20%PEDOT/PSS/EG vs. electric field strength at frequency 1.0 rad/s, strain 3.0%, 27°C, gap 0.760 mm when G'_0 = 54734 Pa.

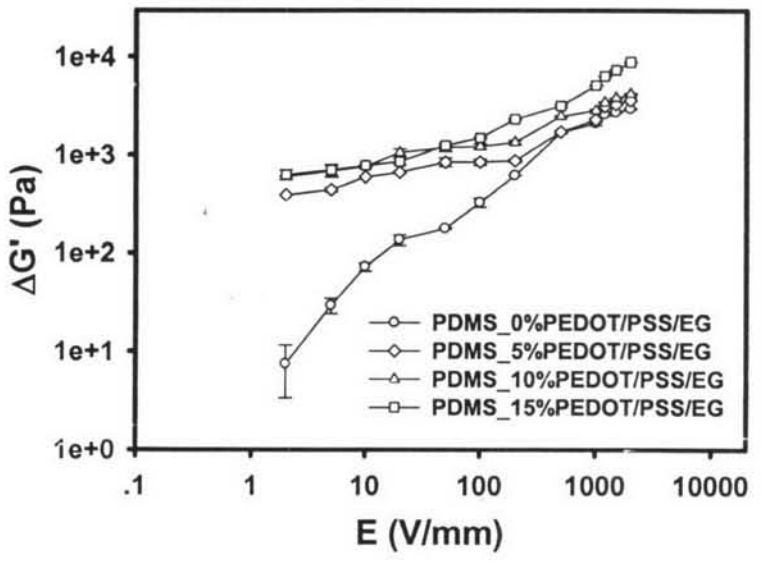

Figure H11 The storage modulus response (ΔG') of pure PDMS and PDMS_PEDOT/PSS/EG blends at various particle concentrations (Φ= 0, 5, 10, 15) vs. electric field strength at frequency 1.0 rad/s, strain 3.0% and at 27°C.

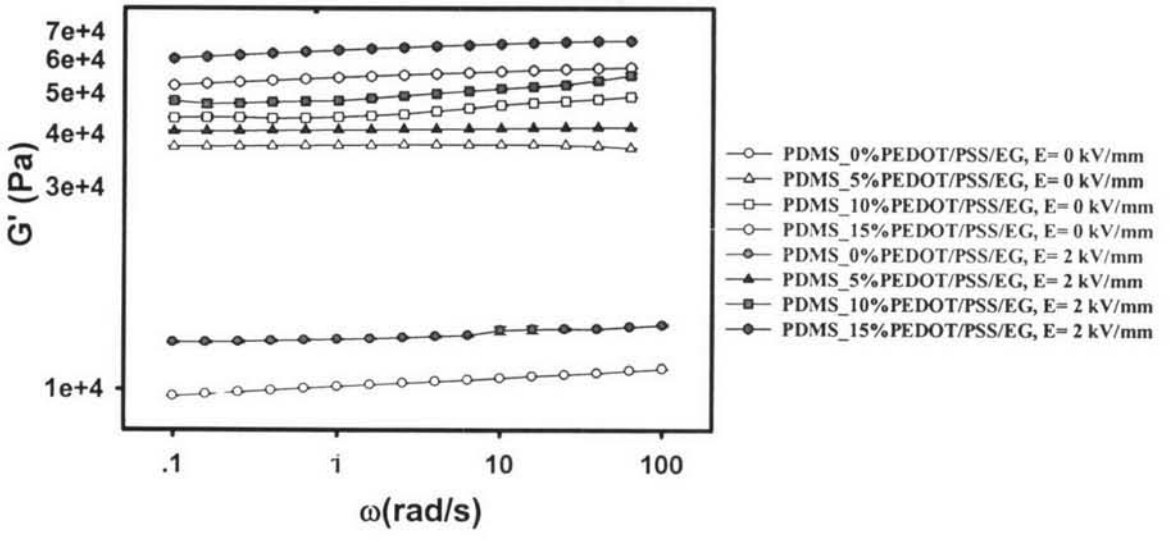

Figure H12 Comparison of the storage modulus of pure PDMS (Φ = 0 %vol.) and PDMS_PEDOT/PSS/EG blends at various particle concentrations (Φ = 5, 10 and 15 %vol.) vs. frequency, strain 3.0%, 27°C at electric field strengths of 0 and 2 kV/mm.

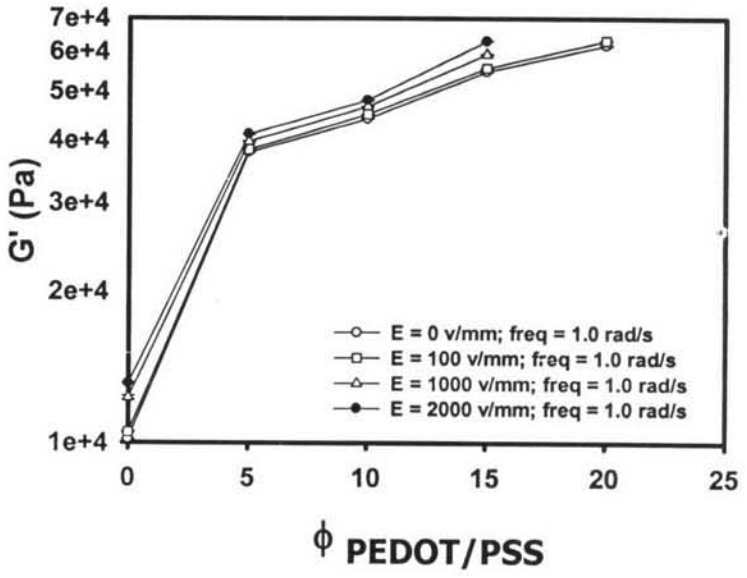

Figure H13 Comparison of the storage modulus response ($\Delta G'$) of pure PDMS and PDMS_PEDOT/PSS/EG blends at various electric field strengths (0, 100, 1000 and 2000 V/mm) vs. particle concentrations (Φ = 0, 5, 10, 15, and 20 %vol.), frequency 1.0 rad/s, strain 3.0% and at 27°C.

CURRICULUM VITAE

Name: Ms. Wijittra Wichiansee

Date of Birth: January 18, 1981

Nationality: Thai

University Education:

2000-2003 Bachelor Degree of Chemistry, Faculty of Science, Khonkaen University, Khonkaen, Thailand